Precision measurements of the cosmological distance scale with upcoming galaxy redshift surveys

Ryuichiro Hada

Collaborators: Daniel Eisenstein (CfA, Harvard)
& Oliver Philcox (Princeton)

20th Nov. 2020, Kavli IPMU Postdoc Colloquium

Contents

Baryon Acoustic Oscillation (BAO)

The baryon-photon plasma propagated as a sound wave before recombination

Over-dense region of baryon (ring shape) got frozen at recombination

The characteristic pattern can be seen in the late-time galaxy distribution

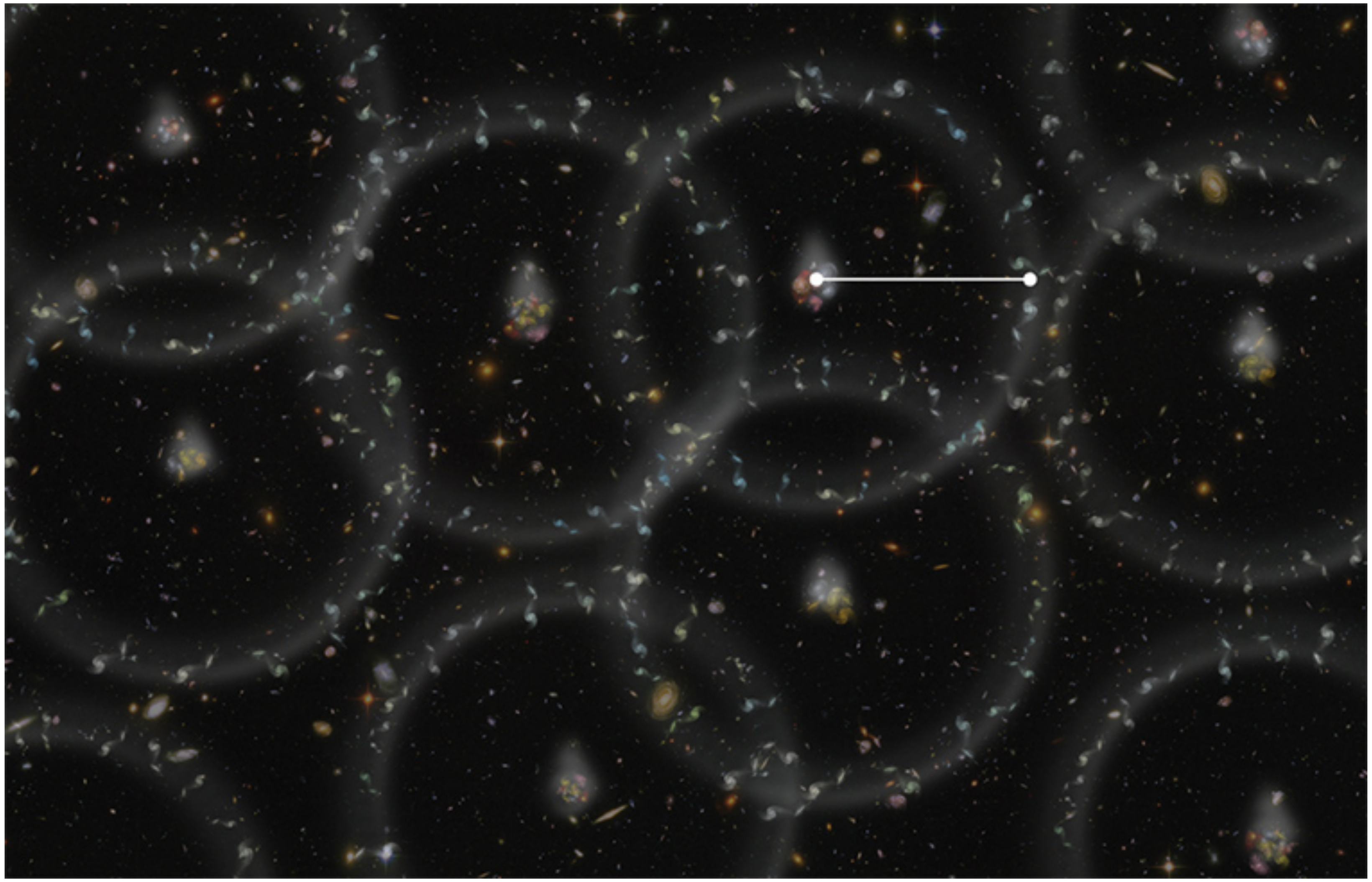

(Credit: Zosia Rostomian, LBNL)

Distance measurement with BAO

The BAO pattern emerges as a peak in the galaxy correlation function

$$\langle n_g(\mathbf{x}_1) n_g(\mathbf{x}_2) \rangle \equiv \bar{n}_g^{\,2}(1 + \xi(|\mathbf{x}_1 - \mathbf{x}_2|))$$

The peak location (r_s) is precisely determined by CMB observations

If we wrongly estimate the separation distances between galaxy pairs, the BAO peak is shifted

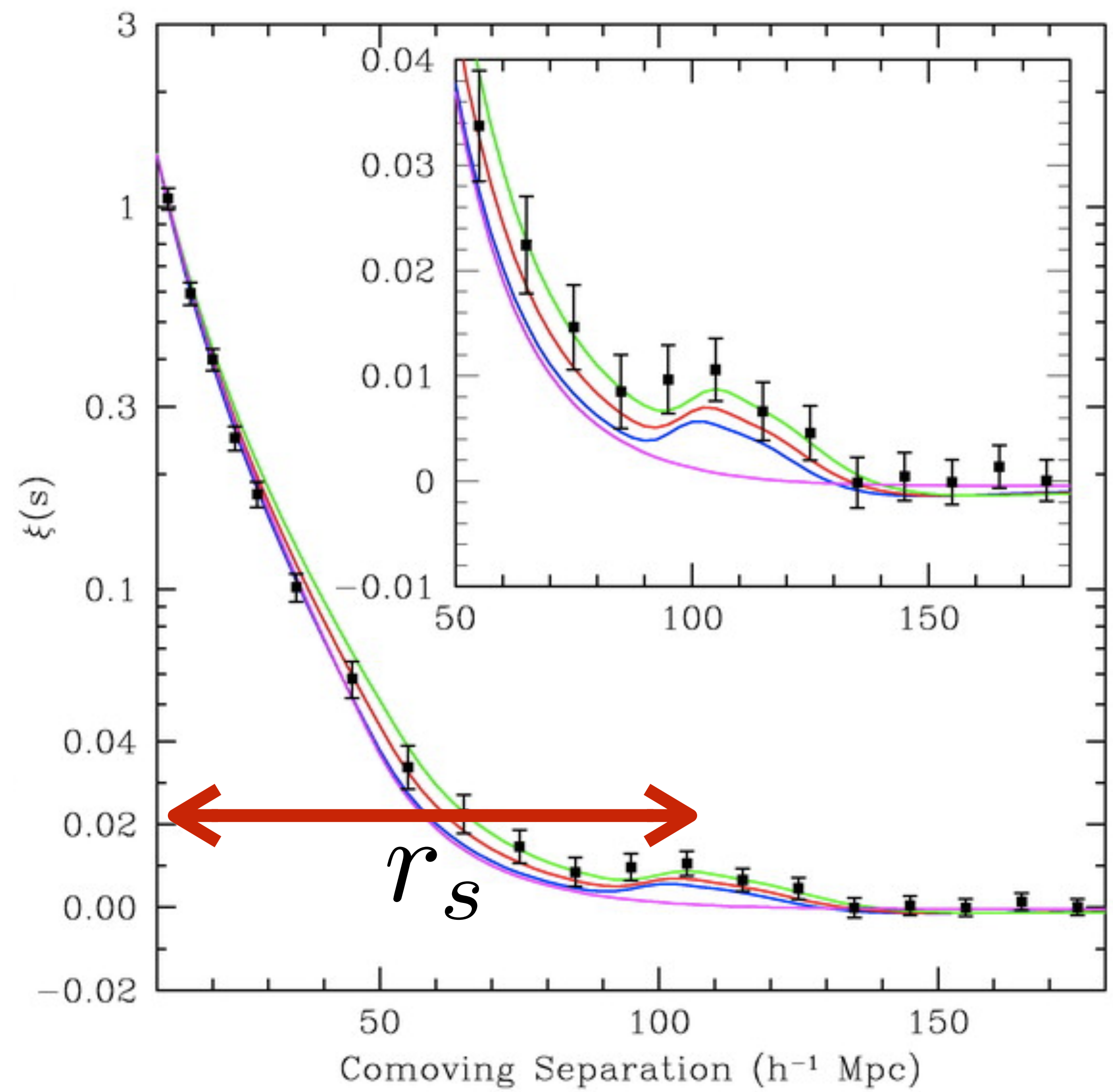

(Eisenstein+ 2005)

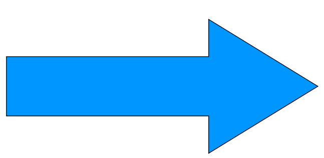

We can measure the cosmological distance scale by focusing the position of BAO peak (*standard ruler*)

Dark energy and the distance scale

(Alam+ 2016)

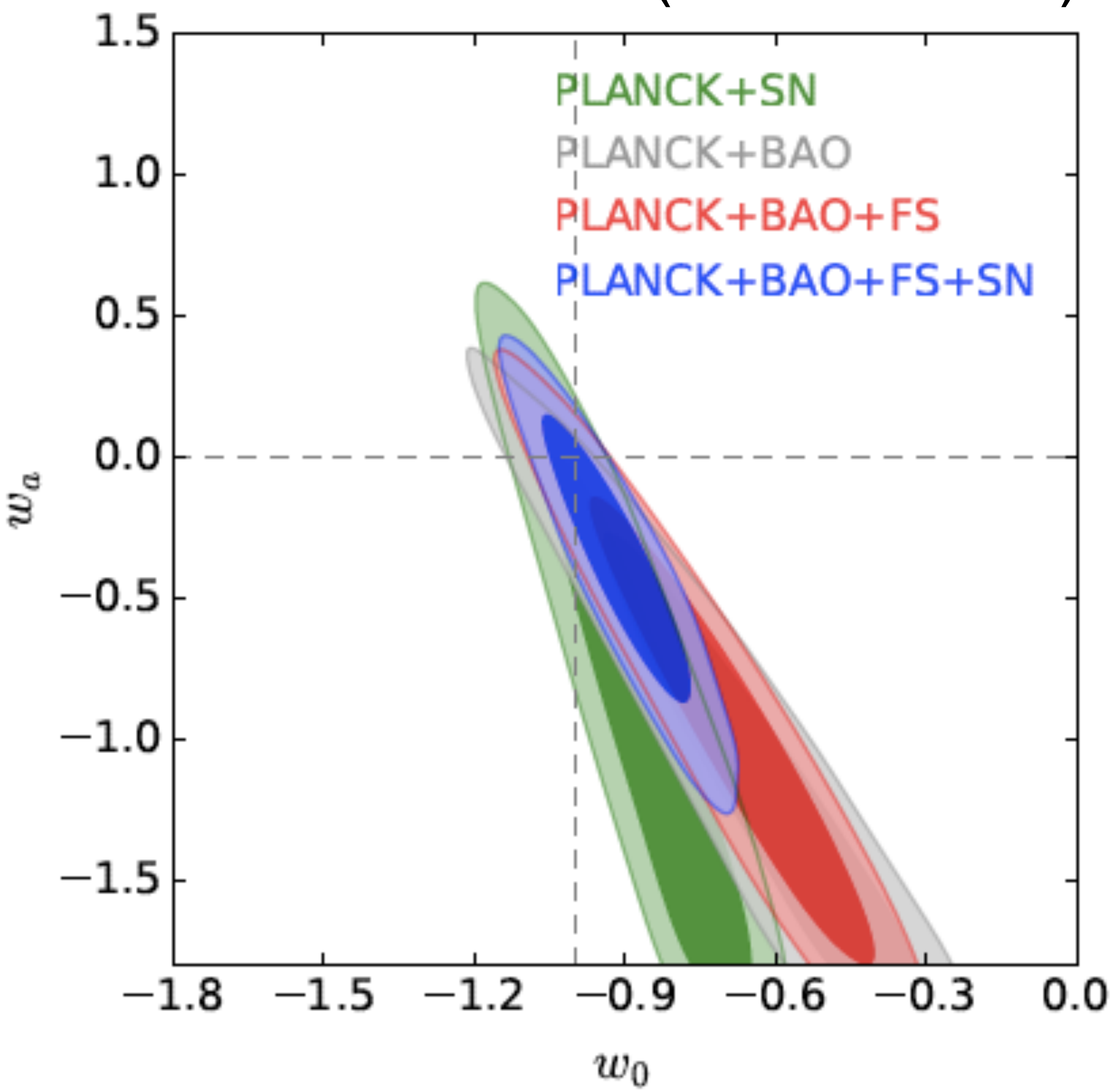

Distances to galaxies depend on the cosmological parameters

line-of-sight

$$\boxed{H(z)}, \boxed{D_{\rm A}(z)}[H_0, \Omega_\Lambda, w, ...]$$

perpendicular

Eq. of state for DE: $p_\Lambda = w\rho_\Lambda$

$w < -1/3$: for accelerated expansion

$w(a) = w_0 + (1-a)w_a$: in general

need to measure the distance scale more precisely to understand the property of DE

Degradation of the BAO signature

1). Peak broadening

Peculiar velocities of galaxies smear out the BAO feature

2). Redshift space distortion (RSD)

The movements along the line of sight affect on the redshift determination (observed in “redshift space”)

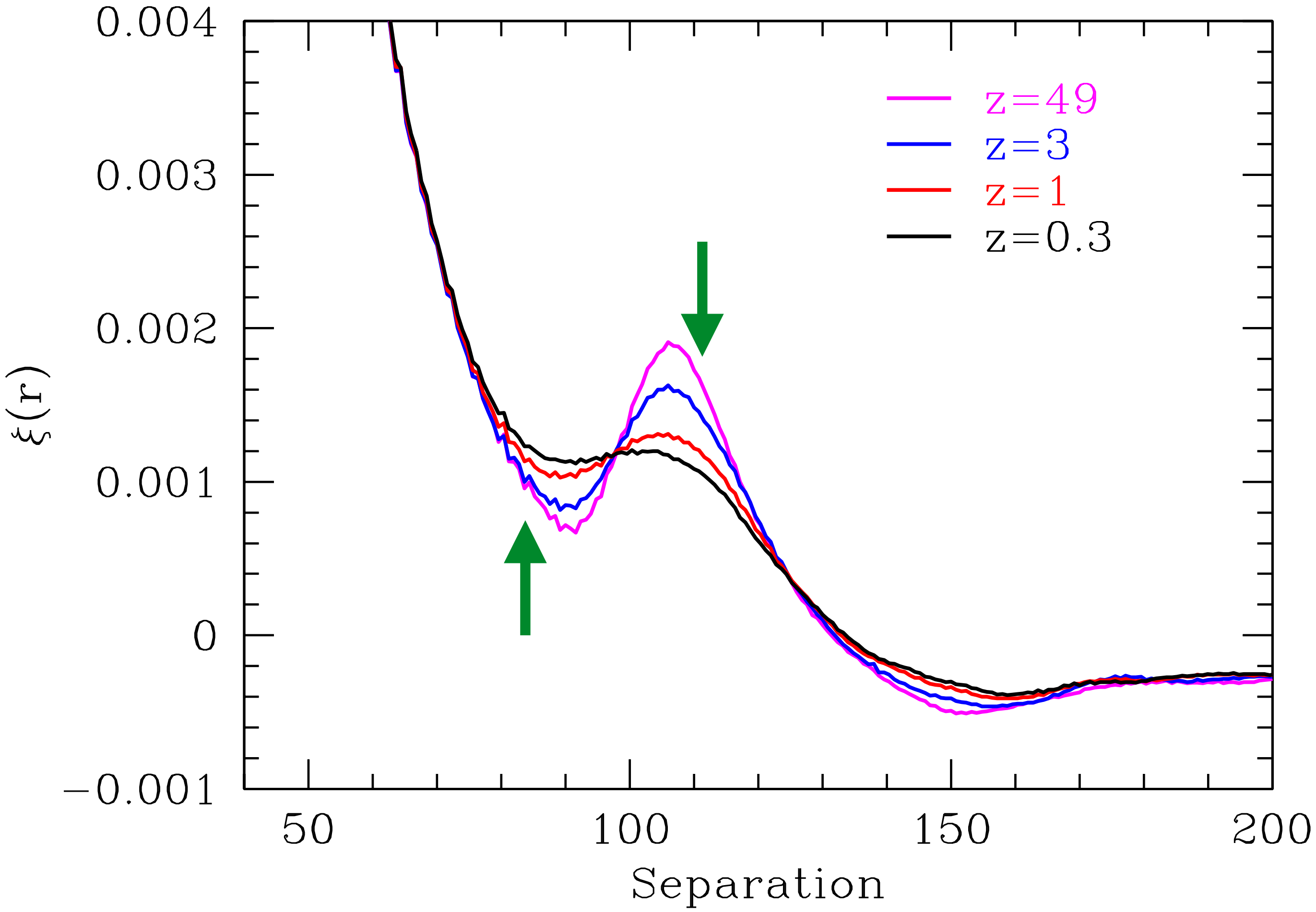

(Seo & Eisenstein 2005)

increasing the distance errors

need to handle with nonlinear effects…
But this degradation is mainly caused by large-scale flow

Reconstruction of the linear density field

1). estimate the displacement from the observed density filed

Zeldovich approximation (ZA) $\tilde{\mathrm{S}}^{(1)}(\mathbf{k}) = \frac{i\mathbf{k}}{k^2}\tilde{\delta}_{\mathrm{L}}(\mathbf{k})G(k)$ (in Fourier space)

$$\delta \equiv \frac{\rho - \bar{\rho}}{\bar{\rho}}$$

$$G(k) = \exp[-0.5k^2\Sigma^2]$$

smoothing scale

2). shift galaxy particles and uniform random particles by that

Galaxy: $\mathbf{S}^{(s)}(\mathbf{q}, t) = \mathbf{S}^{(1)} + f(\mathbf{S}^{(1)} \cdot \hat{\mathbf{z}})\hat{\mathbf{z}}$ Redshift-space distortion

Random: $\mathbf{S}^{(1)}$

where $f = \frac{d\ln D}{d\ln a}$: Linear growth rate

it's like moving "density contrasts"

Reconstructed correlation function

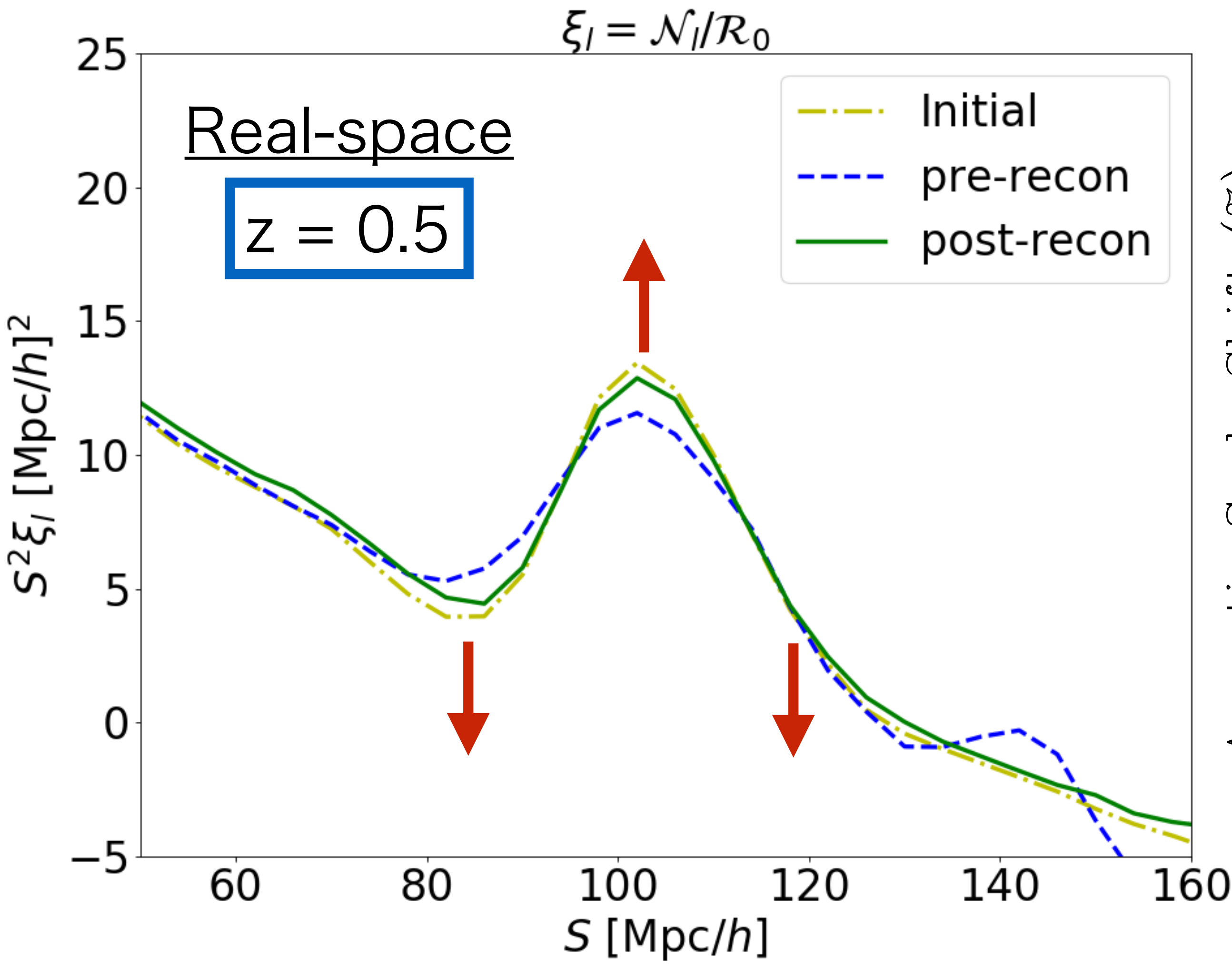

Restored BAO peak

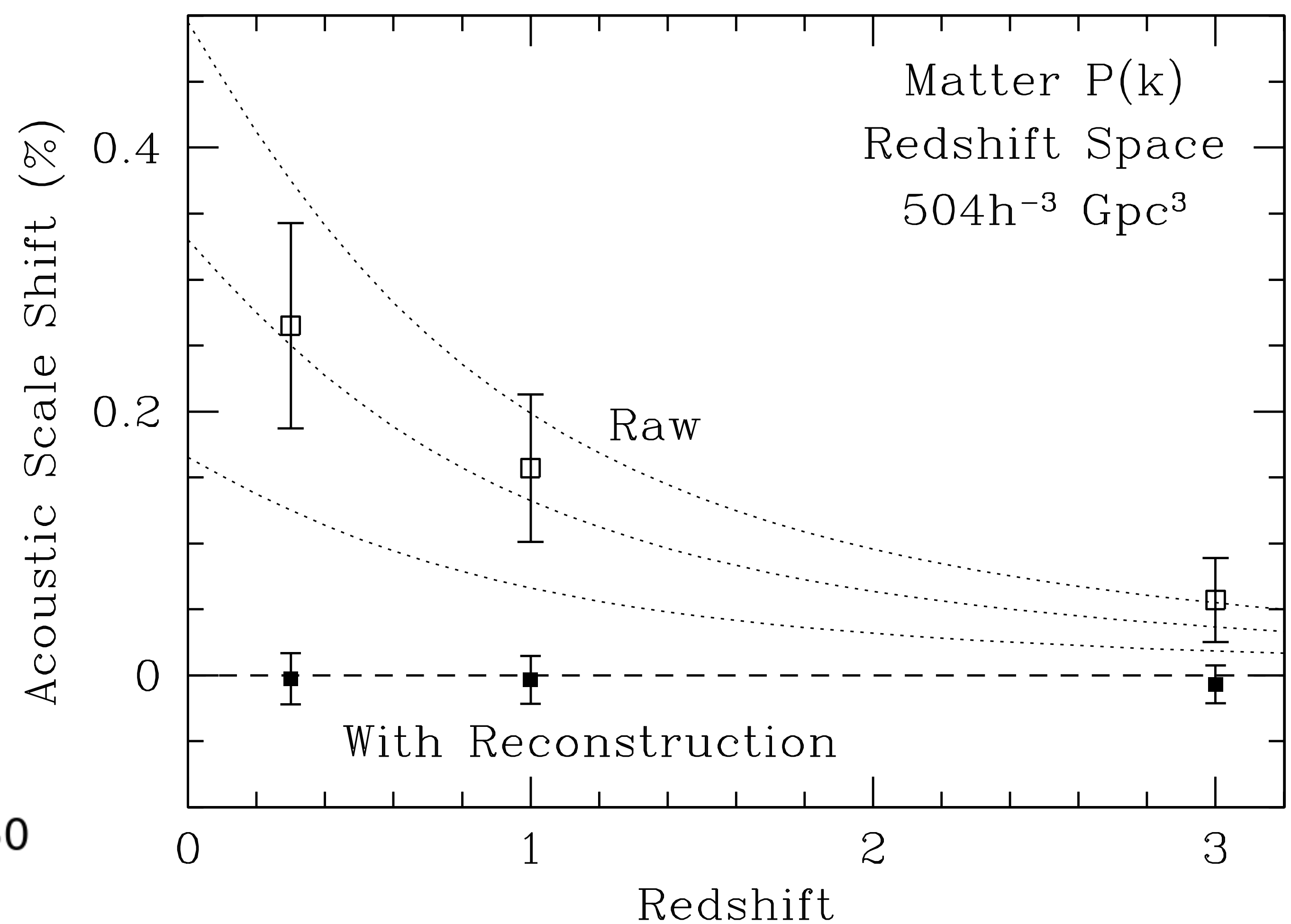

(Seo+ 2010)

The BAO peak is actually recovered

The peak shift is also suppressed

→ improving the statistical precision by a factor of 1.5 - 2

Problems in the standard reconstruction

1). Inconsistency between displacements

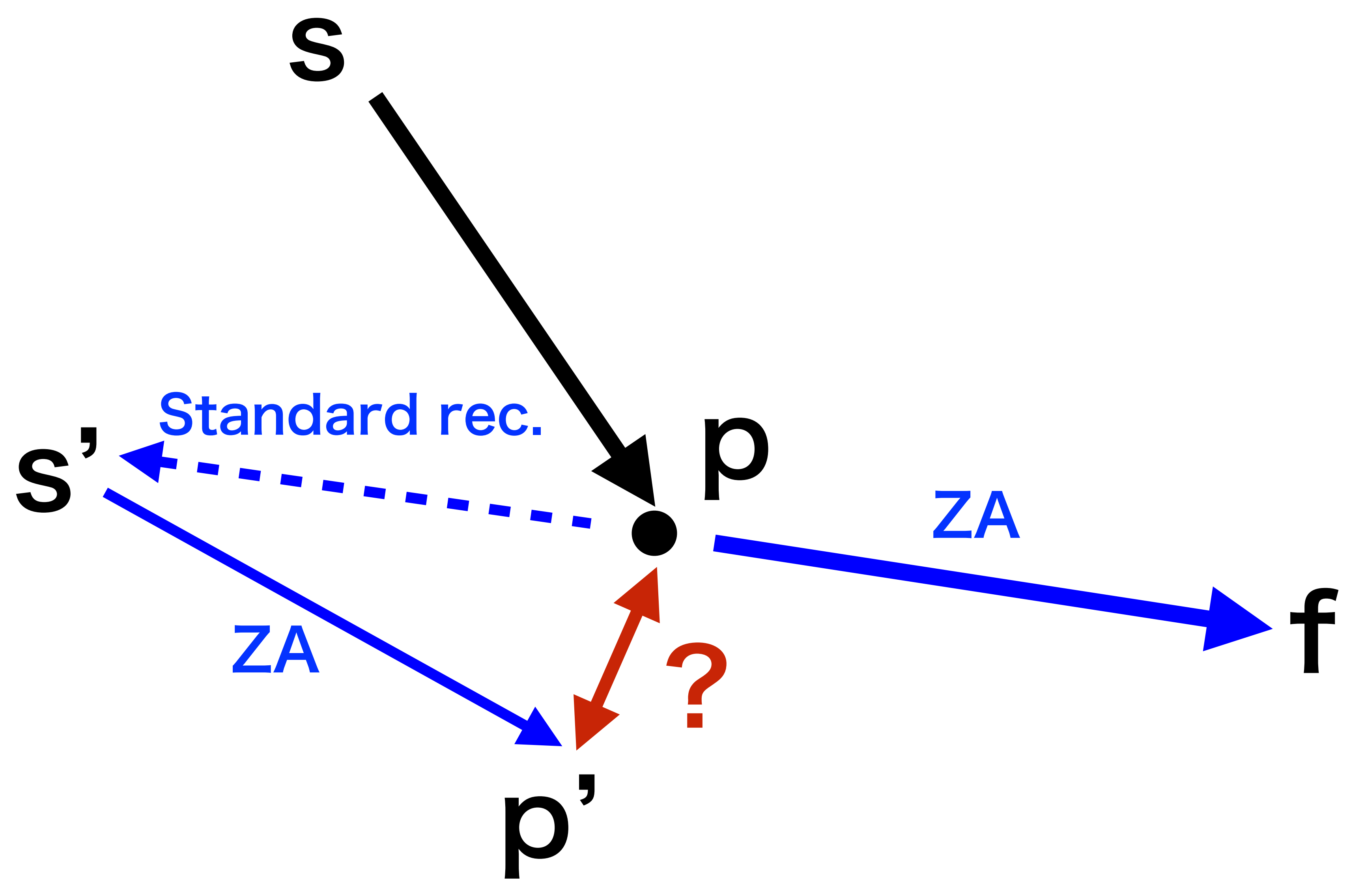

Problems in the standard reconstruction

2). Fake density contrasts

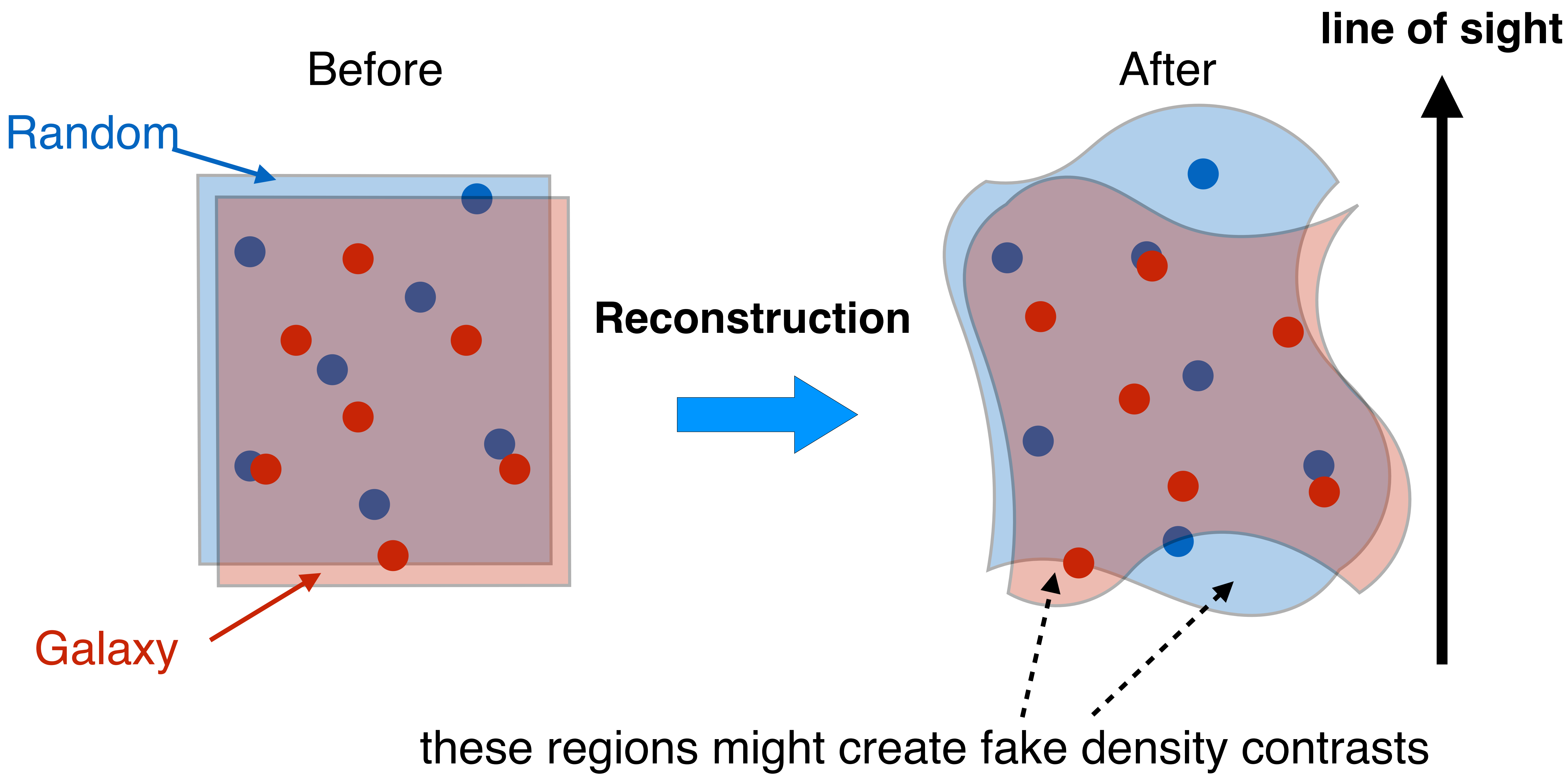

Impact of the smoothing scale

$$\tilde{\mathbf{S}}^{(1)}(\mathbf{k}) = \frac{i\mathbf{k}}{k^2}\tilde{\delta}_{\rm L}(\mathbf{k})G(k)$$

$$G(k) = \exp[-0.5k^2\Sigma^2]$$

smoothing scale

introduced with intent to avoid shot noise effects

but impacts on the results of reconstruction even on large scales (around the BAO peak)

actually affects the (anisotropic) distance measurements

(Vargas-Magaña+ 2017)

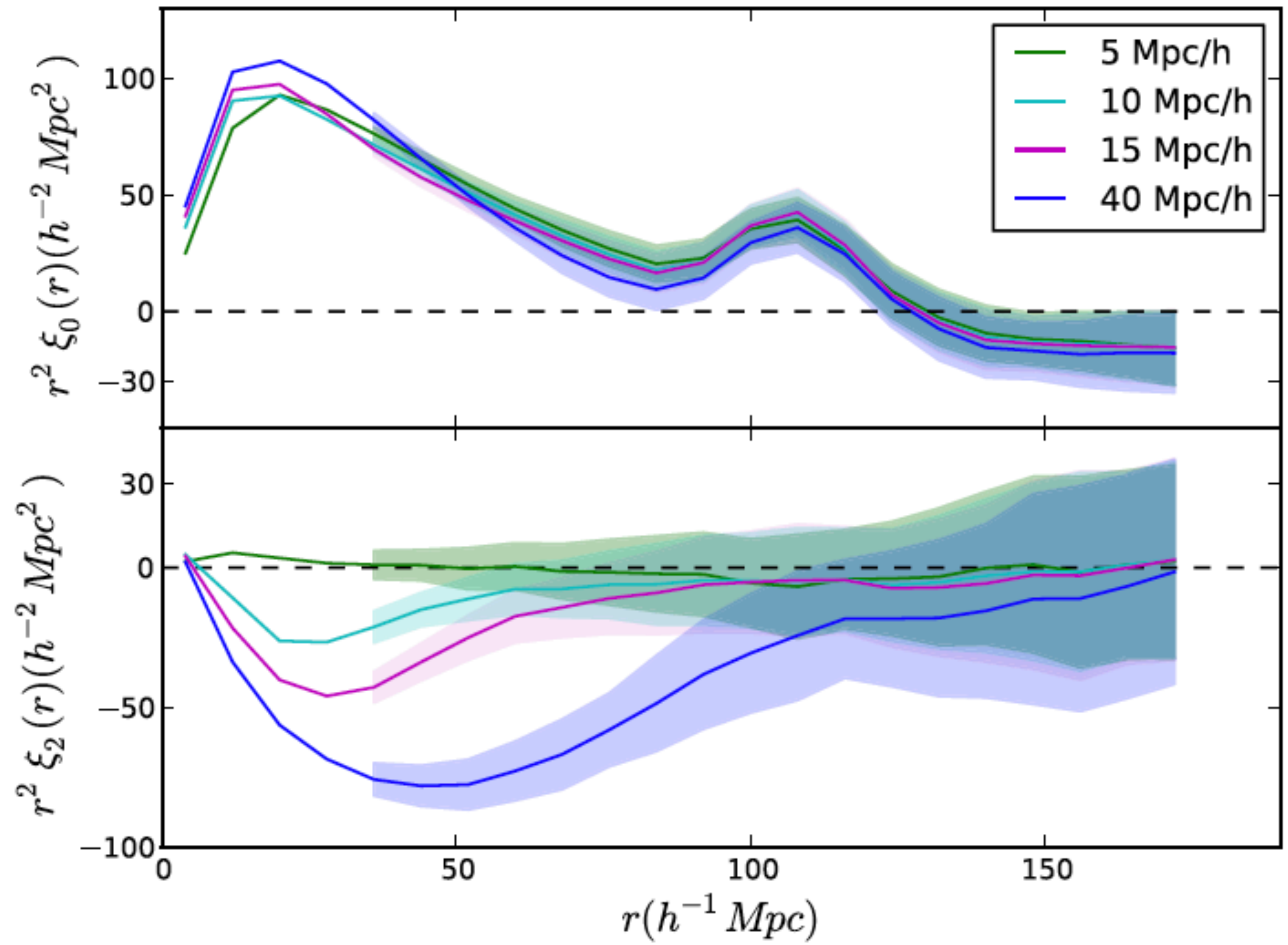

Ongoing galaxy survey projects

<u>DESI</u> Telescope: 4m
Area: 14000 sq. deg.
Redshift: 0.0 - 1.6
Target: LRG, ELG

(DESI Collaboration, 2016)

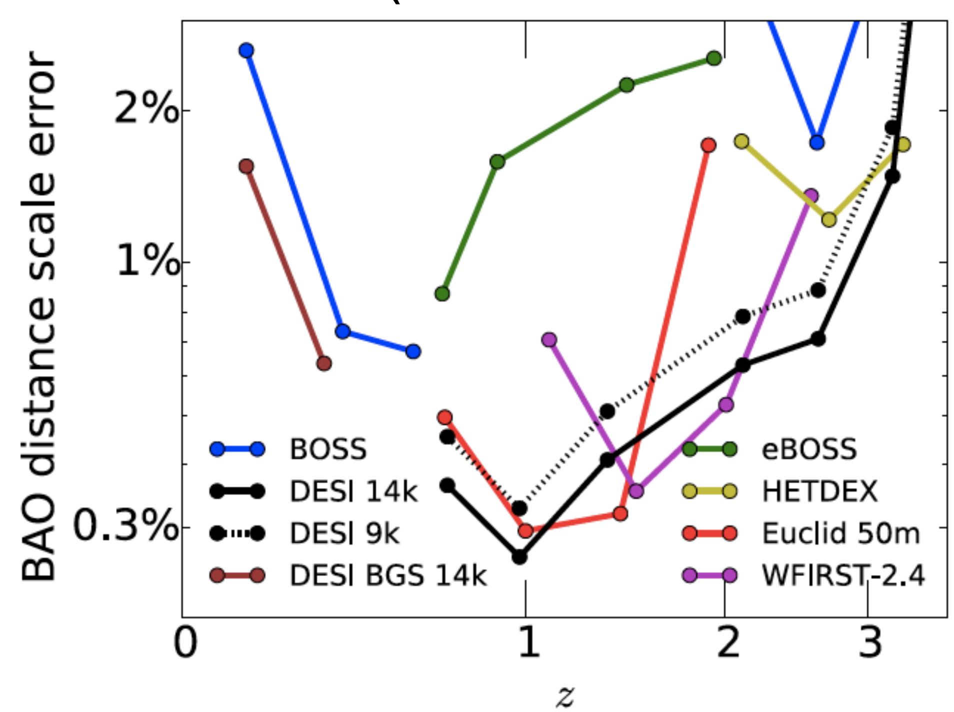

large volume size

→ BAO → Dark energy

<u>PFS</u> Telescope: 8.2m
Area: 1400 sq. deg.
Redshift: 0.6 - 2.4
Target: ELG

(Takada+ 2018)

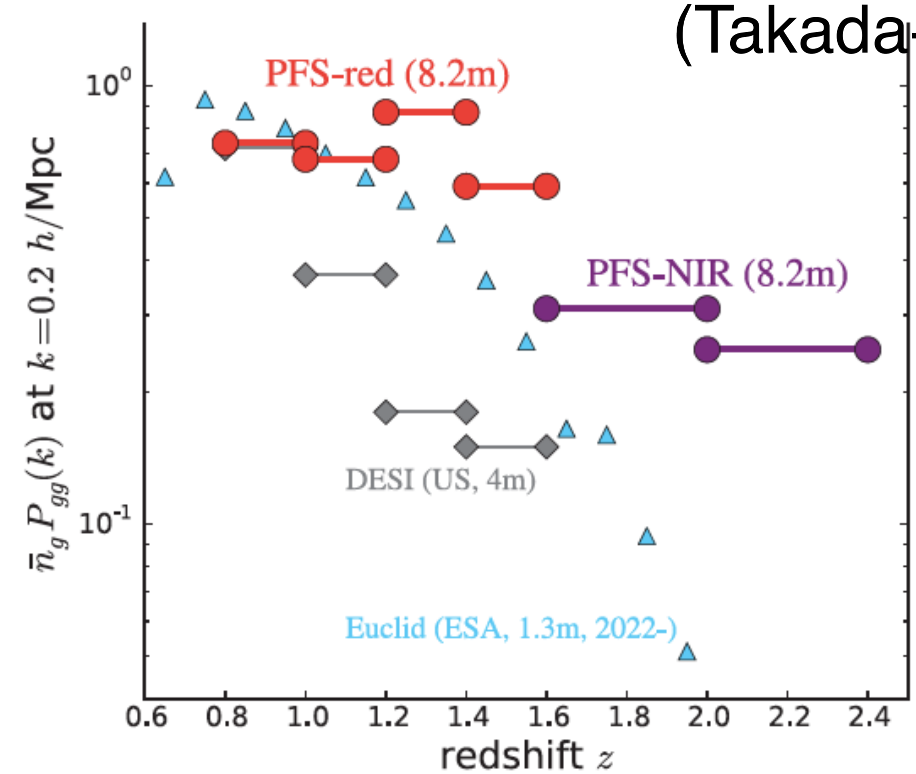

high number density, deeper

→ RSD → neutrino mass

Ongoing galaxy survey projects

DESI Telescope: 4m

Area: 14000 sq. deg.

Redshift: 0.0 - 1.6

Target: LRG, ELG

(DESI Collaboration, 2016)

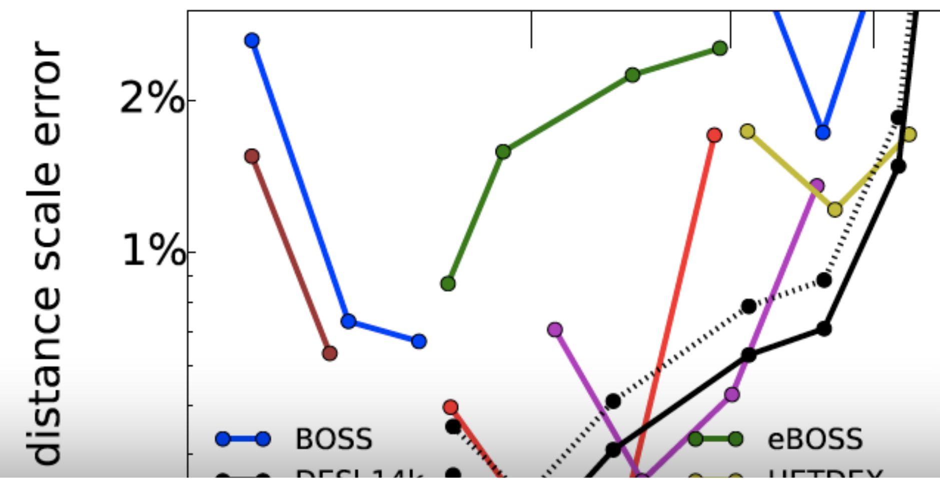

Need to solve the problems in the standard rec. and improve the reliability of the BAO standard ruler !

Telescope: 8.2m

Area: 1400 sq. deg.

Redshift: 0.6 - 2.4

Target: ELG

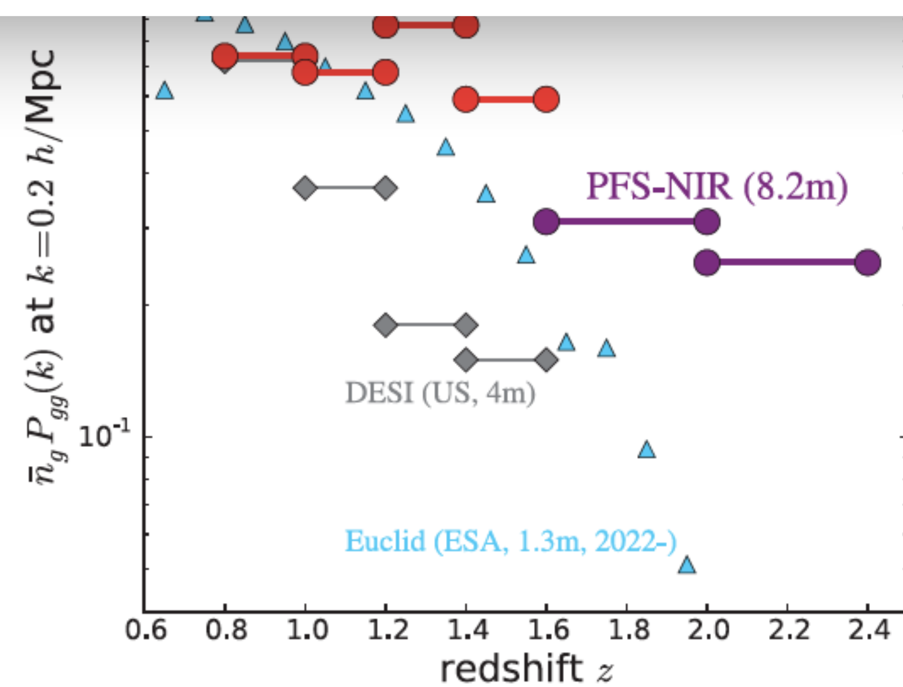

high number density, deeper

→ RSD → neutrino mass

Other methods beyond the standard

Reconstruction algorithm	Stage I: Estimate displacement	Stage II: Estimate linear density
Standard reconstruction [17]	Zeldovich $\hat{\chi}_{\mathrm{ZA}} = \frac{i\boldsymbol{k}}{k^2} W \delta_{\mathrm{NL}}$	$\hat{\delta}_0 = \delta_d[\hat{\chi}_{\mathrm{ZA}}] - \delta_s[\hat{\chi}_{\mathrm{ZA}}]$
Iterative standard rec [53]	Iterative Zeldovich with fixed W	$\hat{\delta}_0 = \delta_d[\hat{\chi}_{\mathrm{ZA}}] - \delta_s[\hat{\chi}_{\mathrm{ZA}}]$
Improved standard rec [37]	Zeldovich and iterative Newton-Raphson	$\hat{\delta}_0 = \hat{\delta}_\chi = \boldsymbol{\nabla} \cdot \hat{\chi}$
Standard rec with pixels [54, 55]	Zeldovich $\hat{\chi}_{\mathrm{ZA}} = \frac{i\boldsymbol{k}}{k^2} W \delta_{\mathrm{NL}}$	Move pixels instead of galaxies
Eulerian growth-shift rec [56]	Zeldovich $\hat{\chi}_{\mathrm{ZA}} = \frac{i\boldsymbol{k}}{k^2} W \delta_{\mathrm{NL}}$	$\hat{\delta}_0 = \delta_{\mathrm{NL}} - \hat{\chi}_{\mathrm{ZA}} \cdot \boldsymbol{\nabla}\delta - \delta^2$
Nonlinear isobaric rec [57, 58]	Solve diff. eqn. with multigrid algorithm	$\hat{\delta}_0 = \hat{\delta}_\chi = \boldsymbol{\nabla} \cdot \hat{\chi}$
New $\mathcal{O}(1)$ rec	Iteratively solve $T(k)F_Z[\boldsymbol{\nabla}\cdot\chi] = W\delta_{\mathrm{NL}}$ for χ	$\hat{\delta}_0 = \hat{\delta}_\chi = \boldsymbol{\nabla} \cdot \hat{\chi}$
New $\mathcal{O}(2)$ rec	Iteratively solve $T(k)F_Z[\boldsymbol{\nabla}\cdot\chi] = W\delta_{\mathrm{NL}}$ for χ	$\hat{\delta}_0 = t_1(k)\hat{\delta}_\chi + t_2(k)\int_{\boldsymbol{p}} \kappa_2 \hat{\delta}_\chi(\boldsymbol{p})\hat{\delta}_\chi(\boldsymbol{k}-\boldsymbol{p})$
Extended std rec [appdx. B]	Iteratively solve $T(k)F_Z[\boldsymbol{\nabla}\cdot\chi] = W\delta_{\mathrm{NL}}$ for χ	$\hat{\delta}_0 = \delta_d[\hat{\chi}] - \delta_s[\hat{\chi}]$

(Schmittfull+ 2017)

Other methods beyond the standard

Reconstruction algorithm	Stage I: Estimate displacement	Stage II: Estimate linear density
Standard reconstruction [17]	Zeldovich $\hat{\chi}_{\rm ZA} = \frac{i\boldsymbol{k}}{k^2} W \delta_{\rm NL}$	$\hat{\delta}_0 = \delta_d[\hat{\chi}_{\rm ZA}] - \delta_s[\hat{\chi}_{\rm ZA}]$
Iterative standard rec [53]	Iterative Zeldovich with fixed W	$\hat{\delta}_0 = \delta_d[\hat{\chi}_{\rm ZA}] - \delta_s[\hat{\chi}_{\rm ZA}]$
Improved standard rec [37]	Zeldovich and iterative Newton-Raphson	$\hat{\delta}_0 = \hat{\delta}_\chi = \boldsymbol{\nabla} \cdot \hat{\chi}$
Standard rec with pixels [54, 55]	Zeldovich $\hat{\chi}_{\rm ZA} = \frac{i\boldsymbol{k}}{k^2} W \delta_{\rm NL}$	Move pixels instead of galaxies
Eulerian growth-shift rec [56]	Zeldovich $\hat{\chi}_{\rm ZA} = \frac{i\boldsymbol{k}}{k^2} W \delta_{\rm NL}$	$\hat{\delta}_0 = \delta_{\rm NL} - \hat{\chi}_{\rm ZA} \cdot \boldsymbol{\nabla}\delta - \delta^2$
Nonlinear isobaric rec [57, 58]	Solve diff. eqn. with multigrid algorithm	$\hat{\delta}_0 = \hat{\delta}_\chi = \boldsymbol{\nabla} \cdot \hat{\chi}$
New $\mathcal{O}(1)$ rec	Iteratively solve $T(k)F_Z[\boldsymbol{\nabla}\cdot\chi] = W\delta_{\rm NL}$ for χ	$\hat{\delta}_0 = \hat{\delta}_\chi = \boldsymbol{\nabla} \cdot \hat{\chi}$
New $\mathcal{O}(2)$ rec	Iteratively solve $T(k)F_Z[\boldsymbol{\nabla}\cdot\chi] = W\delta_{\rm NL}$ for χ	$\hat{\delta}_0 = t_1(k)\hat{\delta}_\chi + t_2(k)\int_{\boldsymbol{p}} \kappa_2 \hat{\delta}_\chi(\boldsymbol{p})\hat{\delta}_\chi(\boldsymbol{k}-\boldsymbol{p})$
Extended std rec [appdx. B]	Iteratively solve $T(k)F_Z[\boldsymbol{\nabla}\cdot\chi] = W\delta_{\rm NL}$ for χ	$\hat{\delta}_0 = \delta_d[\hat{\chi}] - \delta_s[\hat{\chi}]$

(Schmittfull+ 2017)

Perform the standard reconstruction many times (“Iterative” method)

→ Not guaranteed to converge

Other methods beyond the standard

Reconstruction algorithm	Stage I: Estimate displacement	Stage II: Estimate linear density
Standard reconstruction [17]	Zeldovich $\hat{\chi}_{\rm ZA} = \frac{i\boldsymbol{k}}{k^2} W \delta_{\rm NL}$	$\hat{\delta}_0 = \delta_d[\hat{\chi}_{\rm ZA}] - \delta_s[\hat{\chi}_{\rm ZA}]$
Iterative standard rec [53]	Iterative Zeldovich with fixed W	$\hat{\delta}_0 = \delta_d[\hat{\chi}_{\rm ZA}] - \delta_s[\hat{\chi}_{\rm ZA}]$
Improved standard rec [37]	Zeldovich and iterative Newton-Raphson	$\hat{\delta}_0 = \hat{\delta}_\chi = \boldsymbol{\nabla} \cdot \hat{\chi}$
Standard rec with pixels [54, 55]	Zeldovich $\hat{\chi}_{\rm ZA} = \frac{i\boldsymbol{k}}{k^2} W \delta_{\rm NL}$	Move pixels instead of galaxies
Eulerian growth-shift rec [56]	Zeldovich $\hat{\chi}_{\rm ZA} = \frac{i\boldsymbol{k}}{k^2} W \delta_{\rm NL}$	$\hat{\delta}_0 = \delta_{\rm NL} - \hat{\chi}_{\rm ZA} \cdot \boldsymbol{\nabla}\delta - \delta^2$
Nonlinear isobaric rec [57, 58]	Solve diff. eqn. with multigrid algorithm	$\hat{\delta}_0 = \hat{\delta}_\chi = \boldsymbol{\nabla} \cdot \hat{\chi}$
New $\mathcal{O}(1)$ rec	Iteratively solve $T(k)F_Z[\boldsymbol{\nabla}\cdot\chi] = W\delta_{\rm NL}$ for χ	$\hat{\delta}_0 = \hat{\delta}_\chi = \boldsymbol{\nabla} \cdot \hat{\chi}$
New $\mathcal{O}(2)$ rec	Iteratively solve $T(k)F_Z[\boldsymbol{\nabla}\cdot\chi] = W\delta_{\rm NL}$ for χ	$\hat{\delta}_0 = t_1(k)\hat{\delta}_\chi + t_2(k)\int_{\boldsymbol{p}} \kappa_2 \hat{\delta}_\chi(\boldsymbol{p})\hat{\delta}_\chi(\boldsymbol{k}-\boldsymbol{p})$
Extended std rec [appdx. B]	Iteratively solve $T(k)F_Z[\boldsymbol{\nabla}\cdot\chi] = W\delta_{\rm NL}$ for χ	$\hat{\delta}_0 = \delta_d[\hat{\chi}] - \delta_s[\hat{\chi}]$

(Schmittfull+ 2017)

Perform the standard reconstruction many times ("Iterative" method)

→ Not guaranteed to converge

Estimate the non-linear displacement by solving
the nonlinear partial differential eq. numerically

→ Is the higher-order contribution reliable?

Iterative reconstruction method

(**RH** & Eisenstein, 2018; 2019)

Monaco and Efstathiou (1999)

$$\delta_{\rm res}(\mathbf{q}) = \delta_{\rm L}(\mathbf{q}) - \delta_l(\mathbf{q}) = \delta_{\rm L}(\mathbf{q}) + \nabla\cdot\mathbf{S}_l^{(1)}(\mathbf{q})$$

Continuity eq.

$$\det\left[\delta^{\rm K}_{ab} + S^{(s)}_{l|a,b}\right] = \frac{\rho(\mathbf{q})}{\rho(\mathbf{s})} = \frac{1+\boxed{\delta_{\rm res}(q)}}{1+\delta_s(\mathbf{s})}$$

$$\boxed{\delta_{\rm L}(\mathbf{q},t)} = \boxed{-\mu_1(\mathbf{S}_l^{(1)}) - 1 + (1+\delta_s(\mathbf{s}))\left[1+\mu_1(\mathbf{S}_l^{(s)}) + \mu_2(\mathbf{S}_l^{(s)}) + \mu_3(\mathbf{S}_l^{(s)})\right]}$$

$$\tilde{\mathbf{S}}_l^{(1)}(\mathbf{k}) = \frac{i\mathbf{k}}{k^2}\tilde{\delta}_{\rm L}(\mathbf{k})G(k)$$

Displacements

Redshift-space

$$\mathbf{S}_l^{(s)}(\mathbf{q},t) = \mathbf{S}_l^{(1)} + f(\mathbf{S}_l^{(1)}\cdot\hat{\mathbf{z}})\hat{\mathbf{z}}$$

$$\mathbf{s}(\mathbf{q},t) = \mathbf{q} + \mathbf{S}_l^{(s)}(\mathbf{q},t)$$

Repeat these steps until the linear density field converges

Density fields are defined on a grid cell (no need to move particles)

Iterative reconstruction method

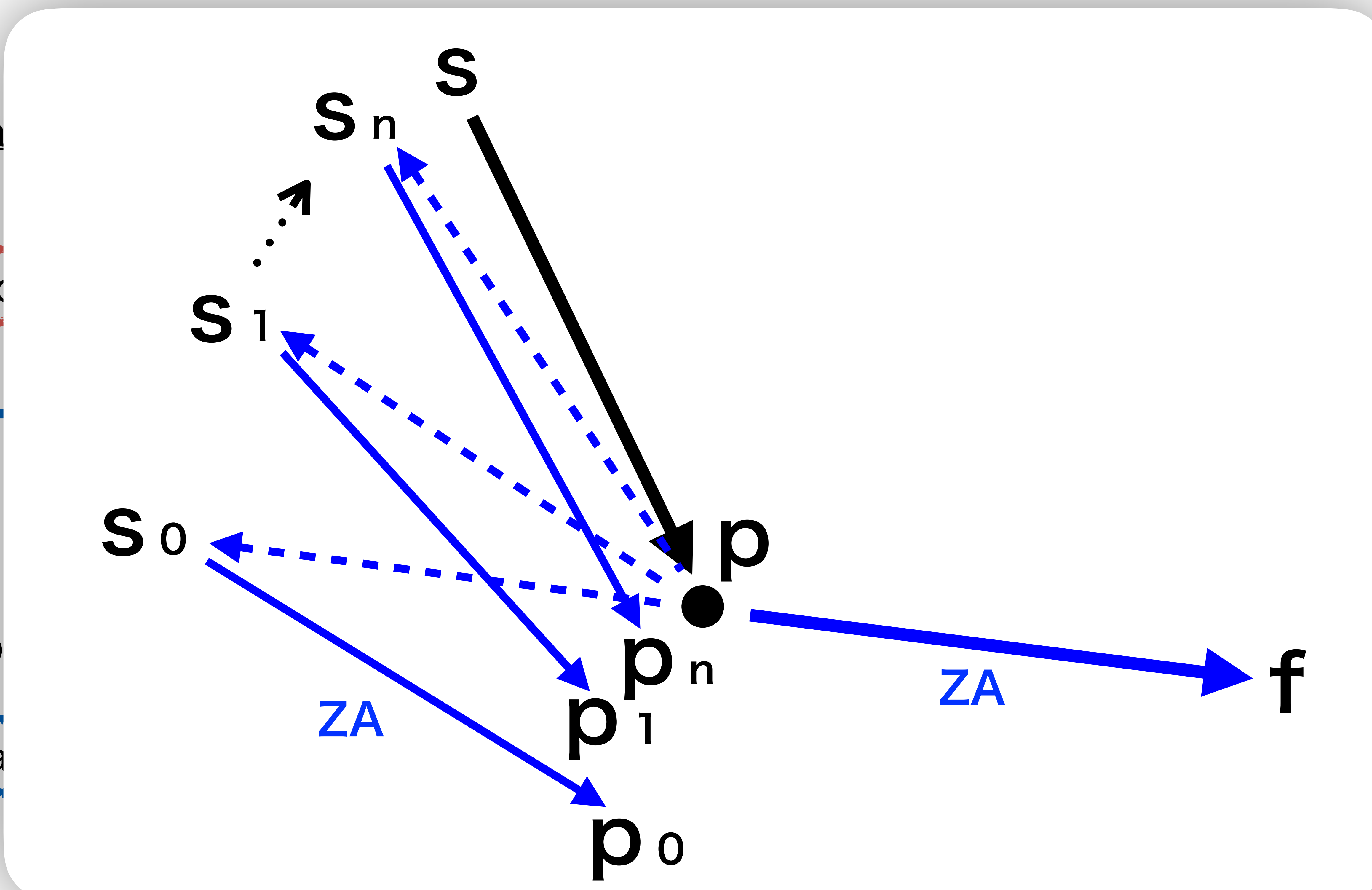

Density fields are defined on a grid cell (no need to move particles)

Iterative reconstruction method

(**RH** & Eisenstein, 2018; 2019)

Monaco and Efstathiou (1999)

$$\delta_{\rm res}(\mathbf{q}) = \delta_{\rm L}(\mathbf{q}) - \delta_l(\mathbf{q}) = \delta_{\rm L}(\mathbf{q}) + \nabla\cdot\mathbf{S}_l^{(1)}(\mathbf{q})$$

Continuity eq. $$\det\left[\delta^{\rm K}_{ab} + S^{(s)}_{l|a,b}\right] = \frac{\rho(\mathbf{q})}{\rho(\mathbf{s})} = \frac{1+\boxed{\delta_{\rm res}(q)}}{1+\delta_s(\mathbf{s})}$$

$$\rightarrow \boxed{\delta_{\rm L}(\mathbf{q},t)} = \boxed{-\mu_1(\mathbf{S}_l^{(1)}) - 1 + (1+\delta_s(\mathbf{s}))\left[1+\mu_1(\mathbf{S}_l^{(s)}) + \mu_2(\mathbf{S}_l^{(s)}) + \mu_3(\mathbf{S}_l^{(s)})\right]}$$

$$\tilde{\mathbf{S}}_l^{(1)}(\mathbf{k}) = \frac{i\mathbf{k}}{k^2}\tilde{\delta}_{\rm L}(\mathbf{k})G(k)$$

Displacements

Redshift-space

$$\mathbf{S}_l^{(s)}(\mathbf{q},t) = \mathbf{S}_l^{(1)} + f(\mathbf{S}_l^{(1)}\cdot\hat{\mathbf{z}})\hat{\mathbf{z}}$$
$$\mathbf{s}(\mathbf{q},t) = \mathbf{q} + \mathbf{S}_l^{(s)}(\mathbf{q},t)$$

Repeat these steps until the linear density field converges

Density fields are defined on a grid cell (no need to move particles)

Performance comparison

N-body simulation

Abacus (Garrison+ 2017), 20 boxes

Box size: 1100 [Mpc/h]

Number of particles: 1440^3

Redshift: z = 0.5

apply reconstruction methods to the matter density field in redshift space

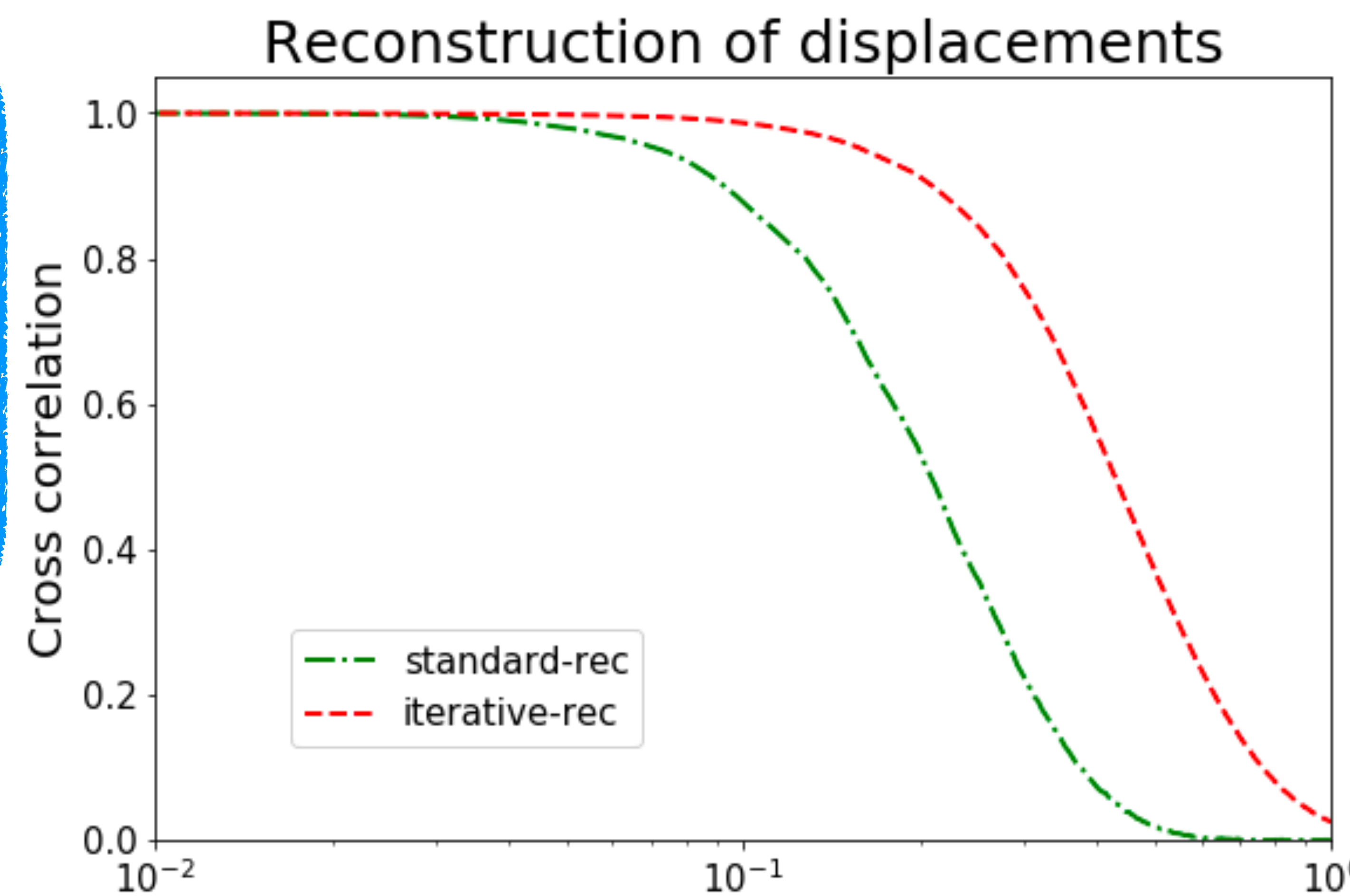

large scale

small scale

iterative method can reconstruct the displacements precisely up to smaller scale

$$r(k) \equiv \frac{\langle \tilde{\mathbf{S}}_{\rm rec} \cdot \tilde{\mathbf{S}}^*_{\rm true} \rangle}{\sqrt{\langle |\tilde{\mathbf{S}}_{\rm rec}|^2 \rangle \langle |\tilde{\mathbf{S}}_{\rm true}|^2 \rangle}}$$

Restoration of the 2-point correlation

<u>Isotropic component</u>

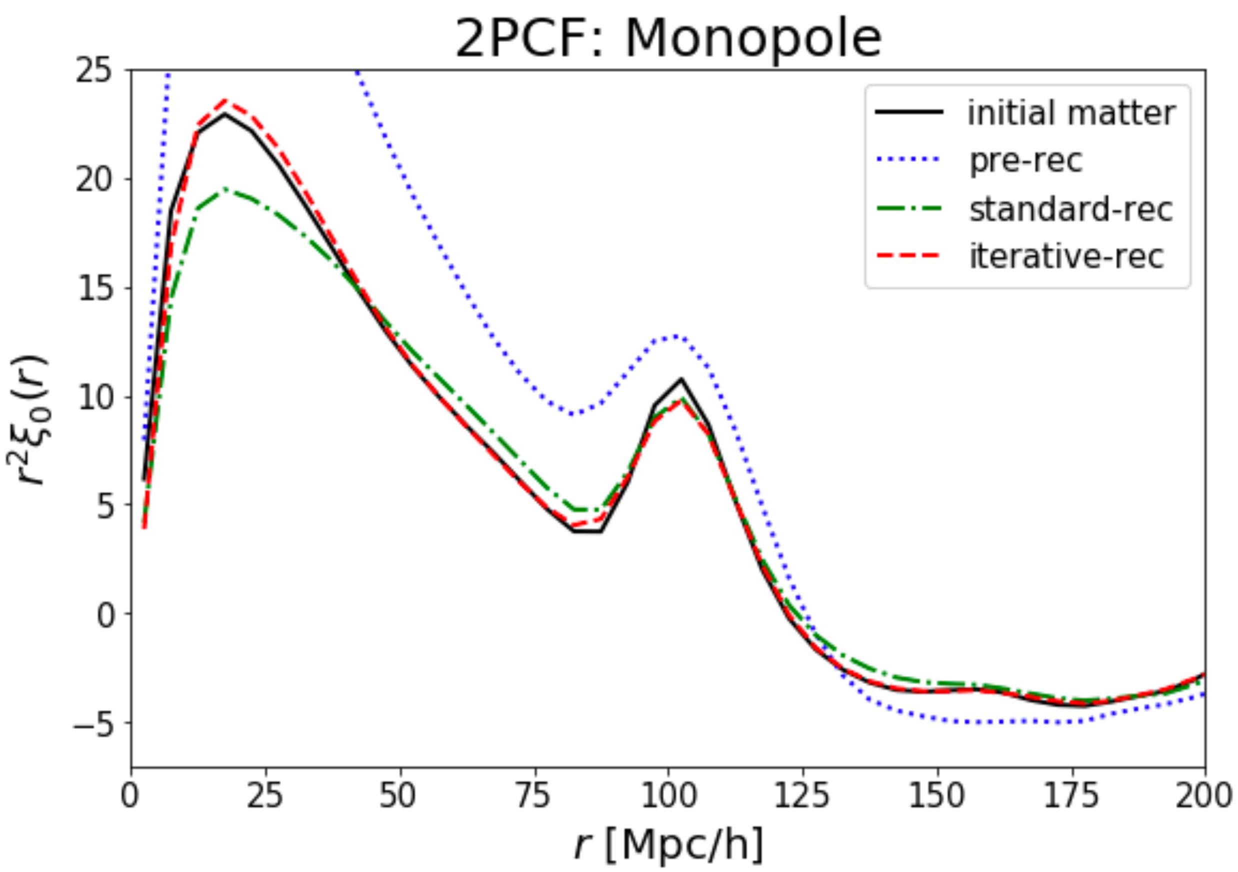

<u>Anisotropic component</u>

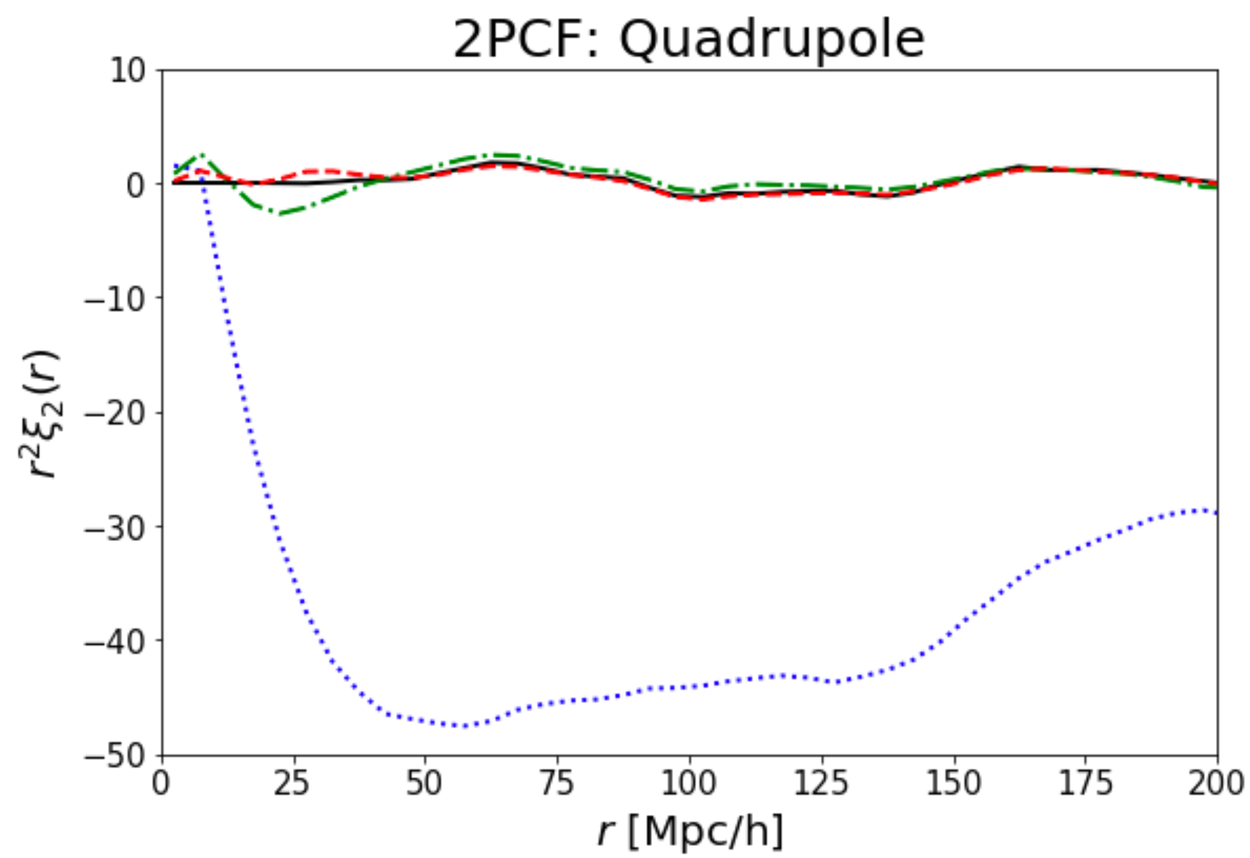

both reconstruction methods restore the 2PCFs roughly in a wide range of r

Restoration of the 2-point correlation

<u>Isotropic component</u>

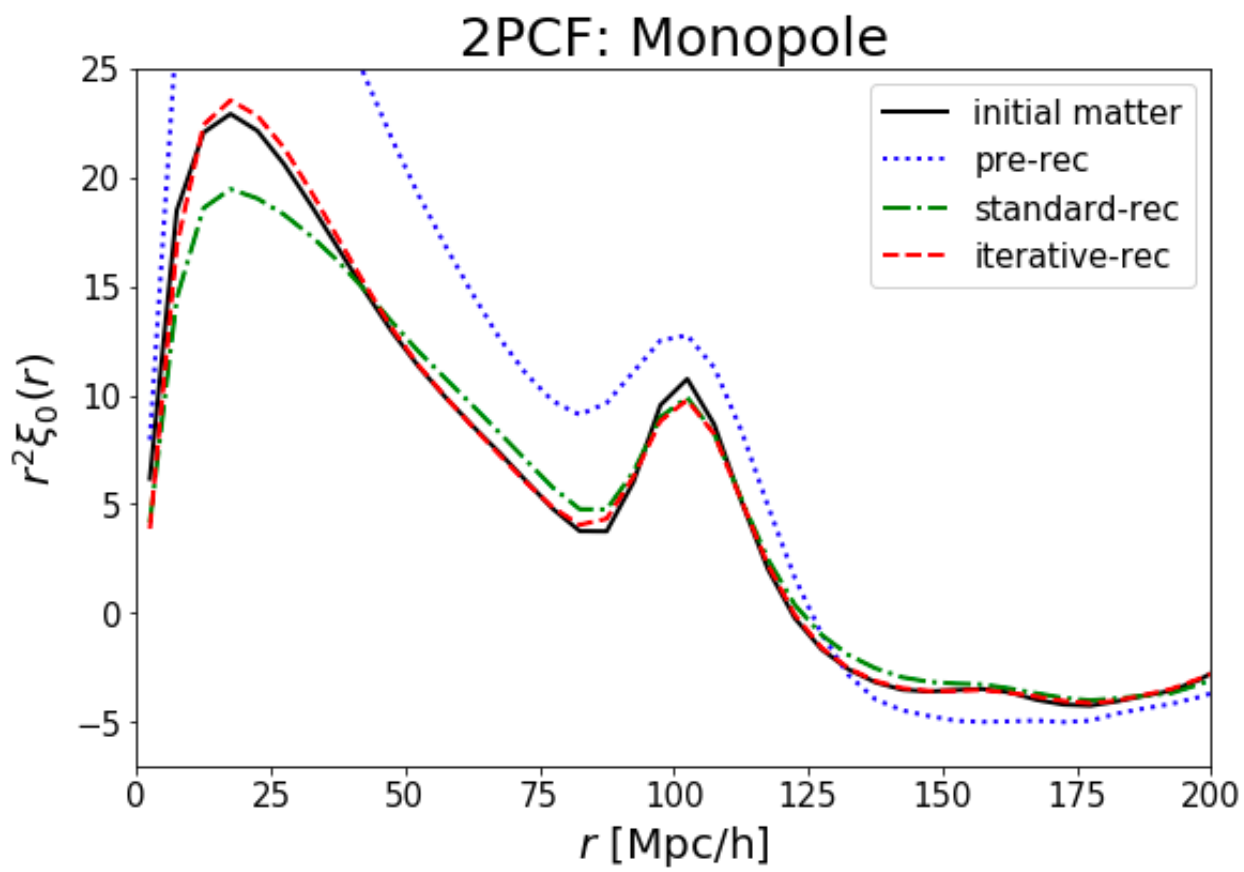

<u>Anisotropic component</u>

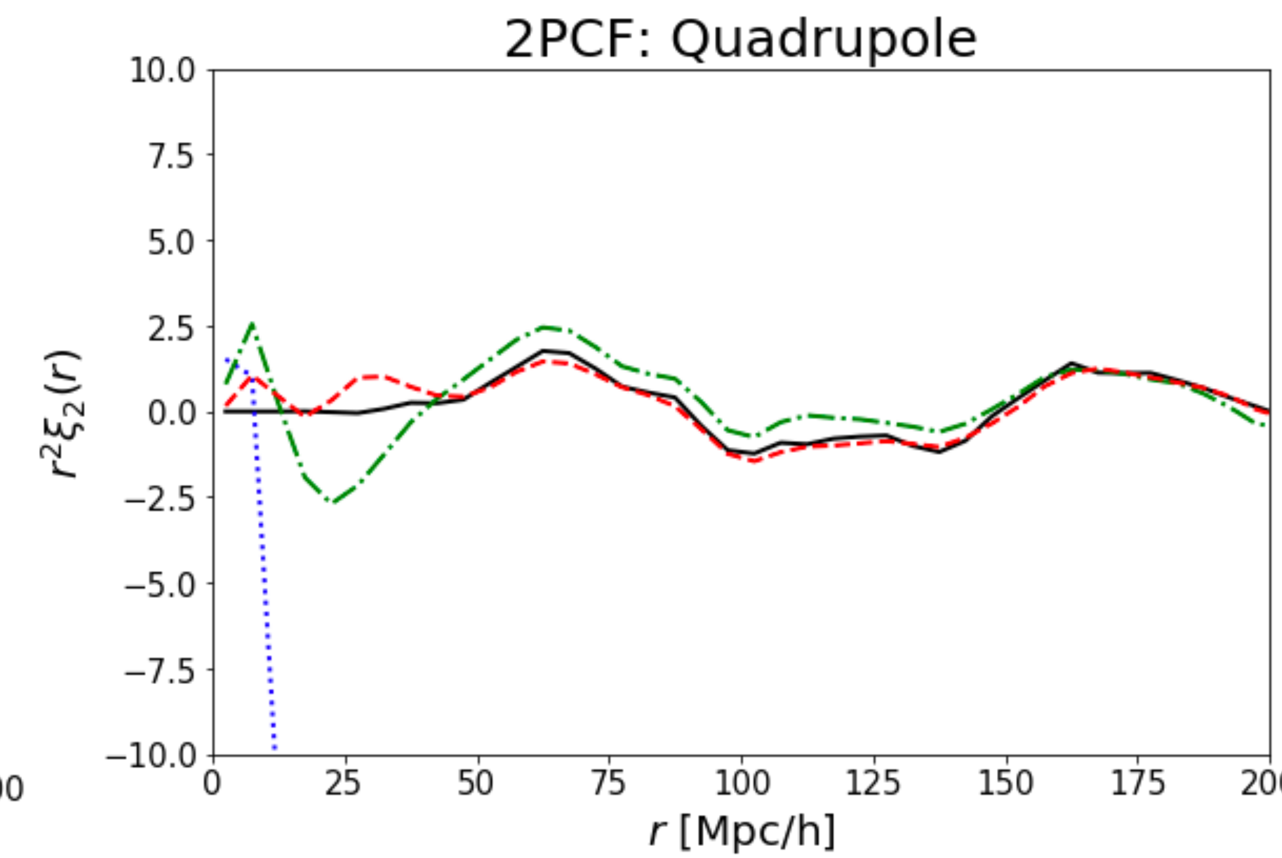

both reconstruction methods restore the 2PCFs roughly in a wide range of r

the iterative method is more consistent with the initial matter especially in the range of $50 < r < 150$ Mpc/h

Dependence on the smoothing scale

(**RH** & Eisenstein, in prep.)

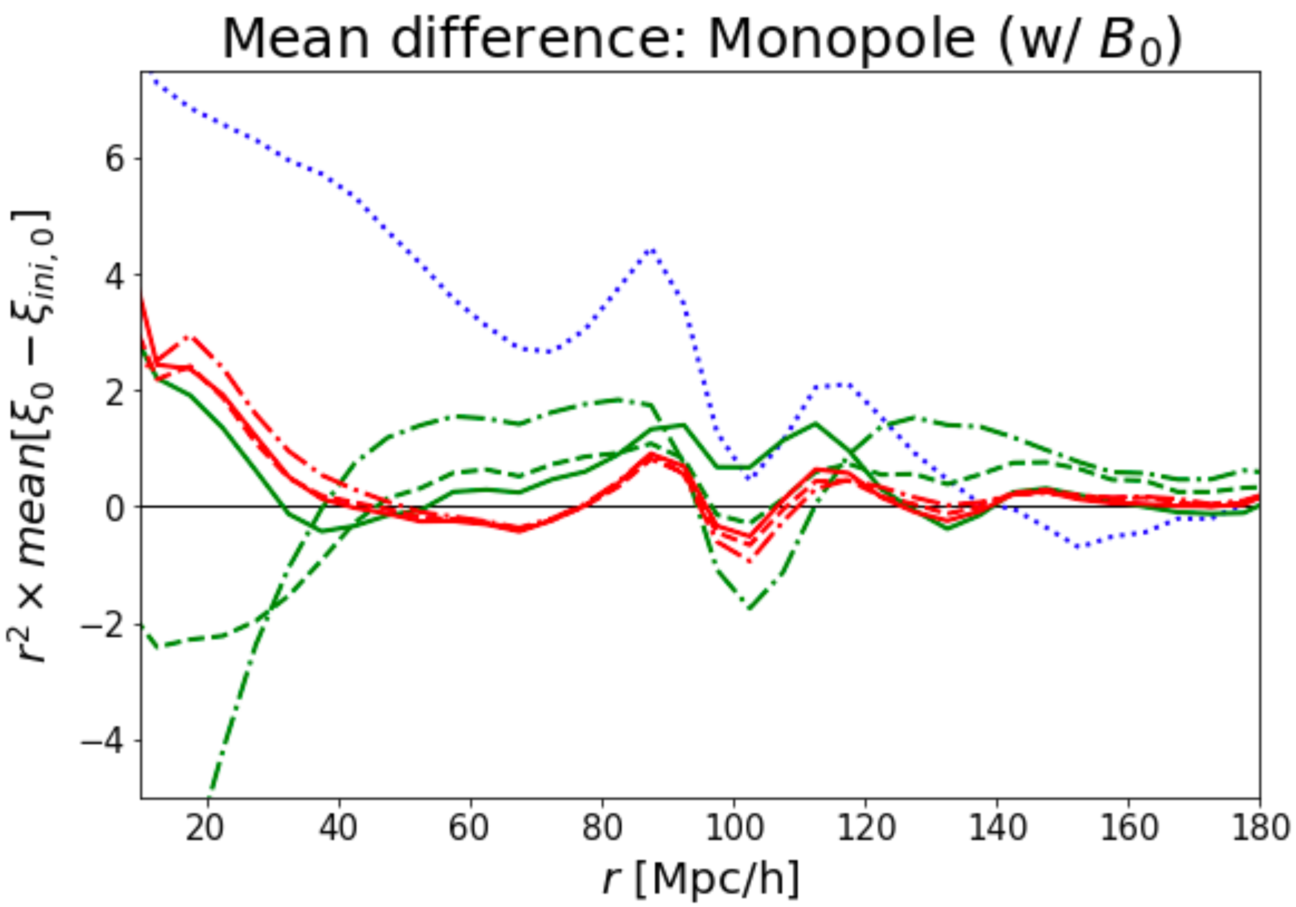

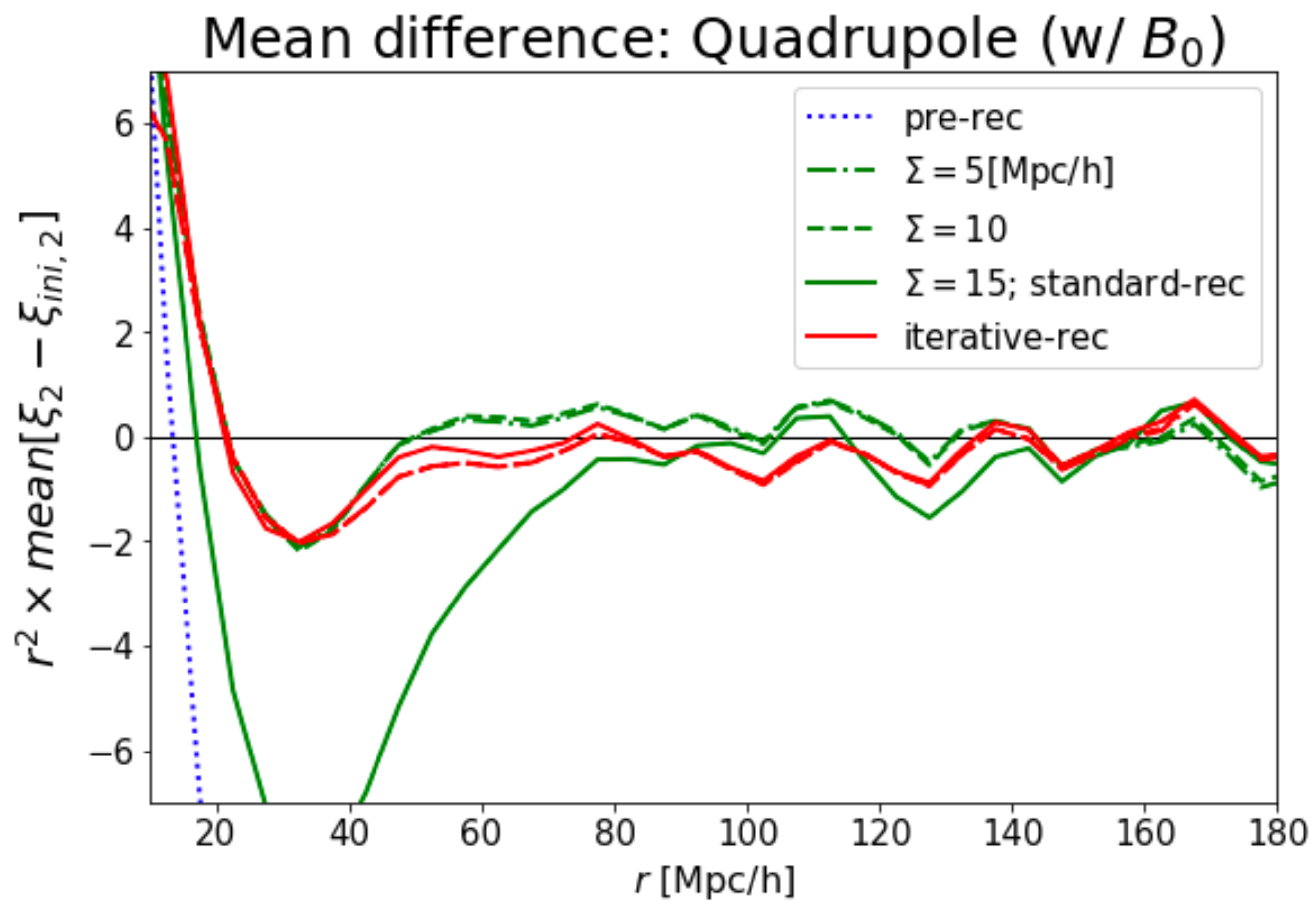

apply reconstruction methods to the galaxy mocks in redshift space

the iterative method is not affected by the smoothing scale

Dependence on the smoothing scale

(**RH** & Eisenstein, in prep.)

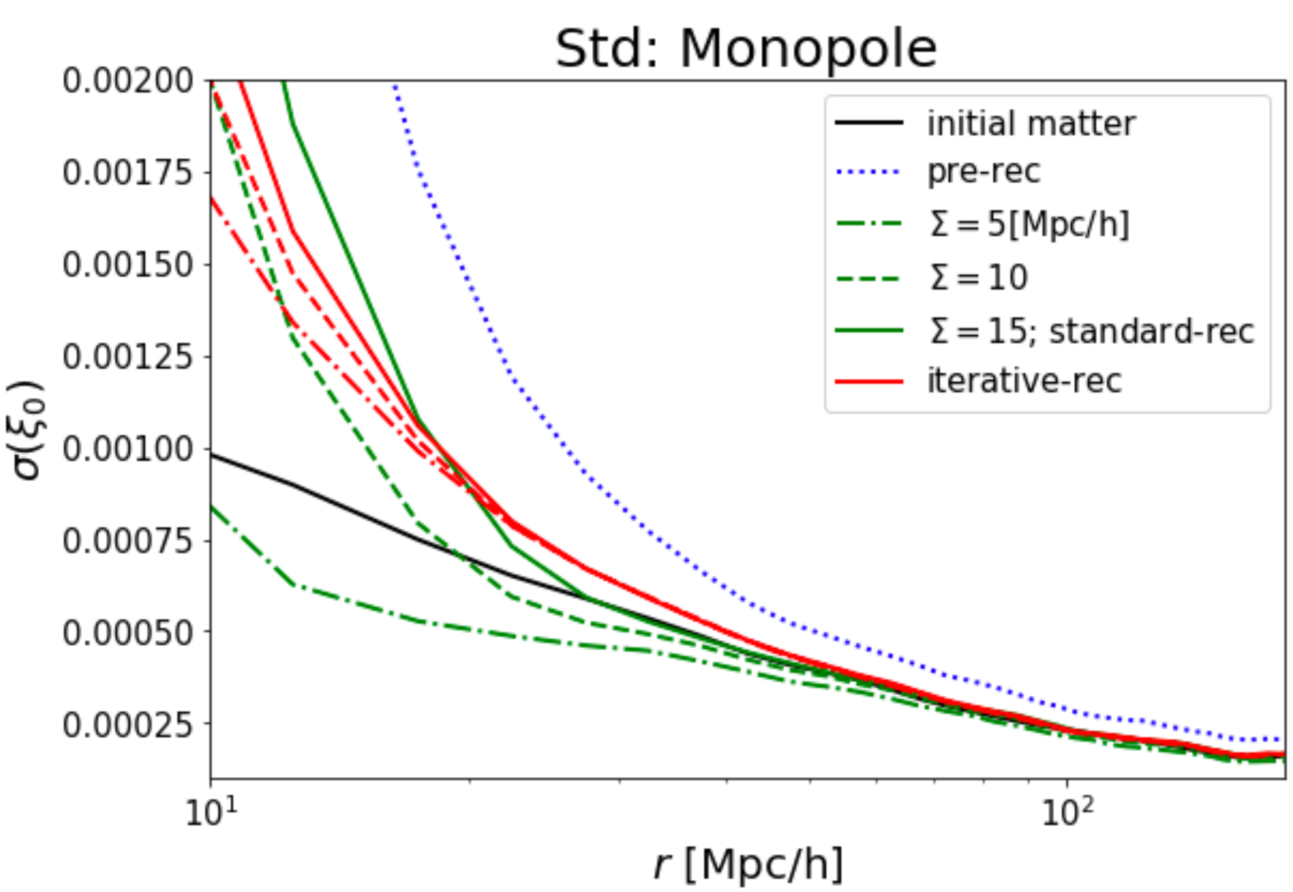

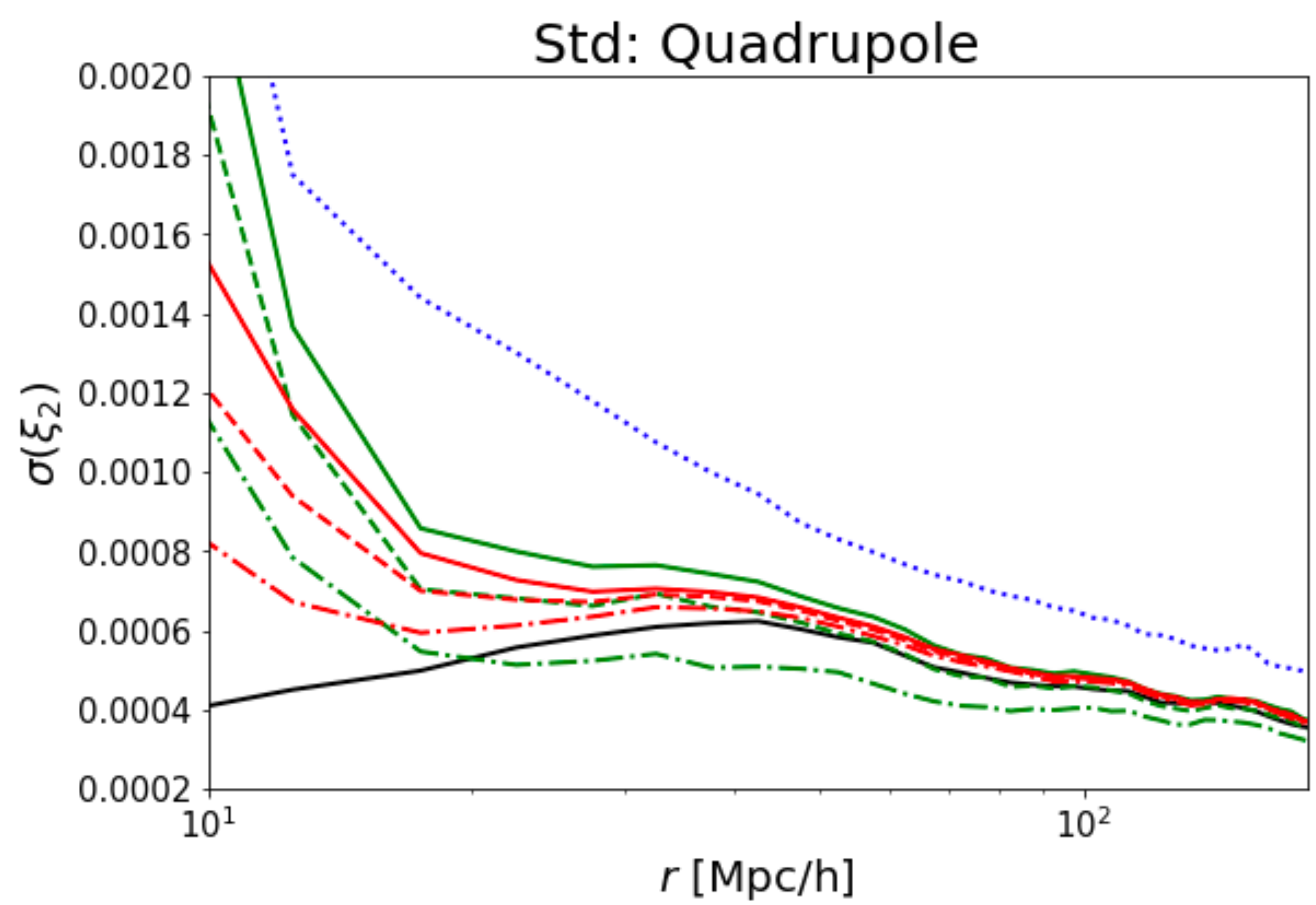

covariance matrices (diagonal part) of the 2PCFs leads to errors of the distance measurement

dependence on the smoothing scale is weaker in the iterative method

Impact on the distance measurements

w/ nuis

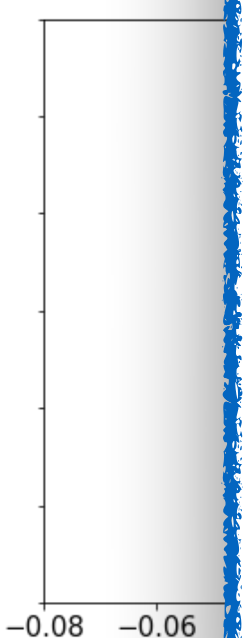

Model template (Ashley *et al.*, 2017)

$$P(k,\mu) = C^2(k,\mu,\Sigma_s)((P_{\rm lin} - P_{\rm nw})e^{-k^2\sigma_v^2} + P_{\rm nw})$$

$$\sigma_v^2 = (1-\mu^2)\Sigma_\perp^2/2 + \mu^2\Sigma_{||}^2/2,$$

$$C(k,\mu,\Sigma_s) = \frac{1+\mu^2\beta(1-S(k))}{(1+k^2\mu^2\Sigma_s^2/2)} \quad S(k) = e^{-k^2\Sigma_r^2/2}$$

$$\xi_{0,\rm mod}(s) = B_0\xi_0(s,\alpha_\perp,\alpha_{||}) + \boxed{A_0(s)}$$

$$\xi_{2,\rm mod}(s) = \frac{5}{2}(B_2\xi_{\mu 2}(s,\alpha_\perp,\alpha_{||}) - B_0\xi_0(s,\alpha_\perp,\alpha_{||})) + \boxed{A_2(s)}$$

where $A_x(s) = a_{x,1}/s^2 + a_{x,2}/s + a_{x,3}$

nuisance parameters

$$\beta = 0$$
$$\Sigma_\perp = \Sigma_{||} = 5 \text{ [Mpc/h]}$$
$$\Sigma_s = \Sigma_r = 0$$
$$B_2 = B_0$$

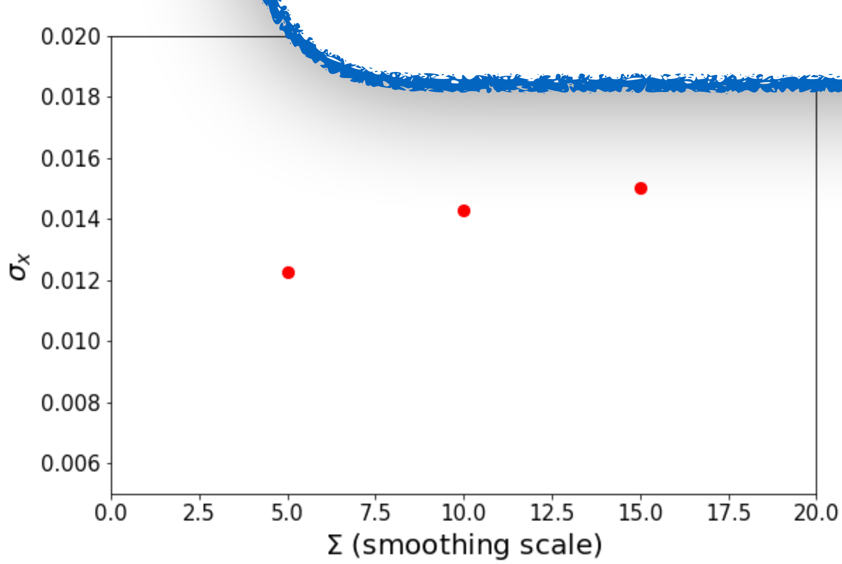

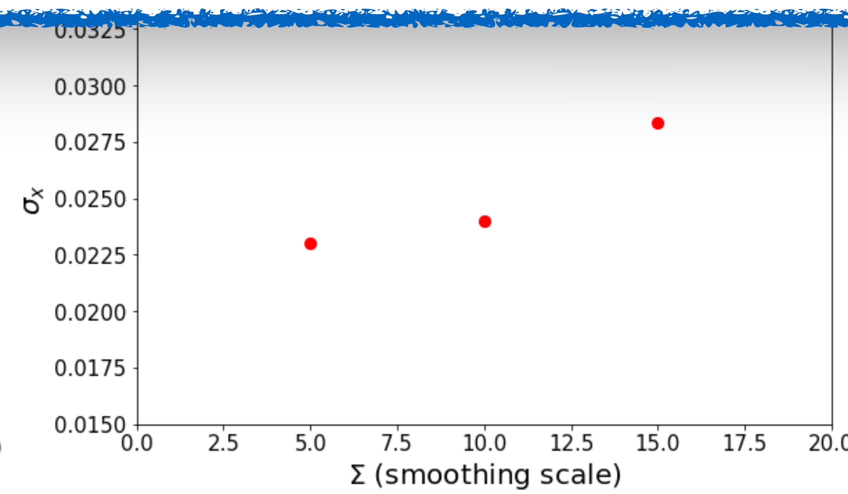

Impact on the distance measurements

w/ nuisance parameters

perpendicular

$$\alpha_\perp = \frac{D_M(z) r_{d,\mathrm{fid}}}{D_M^{\mathrm{fid}}(z) r_d},$$

line-of-sight

$$\alpha_\parallel = \frac{H^{\mathrm{fid}}(z) r_{d,\mathrm{fid}}}{H(z) r_d}$$

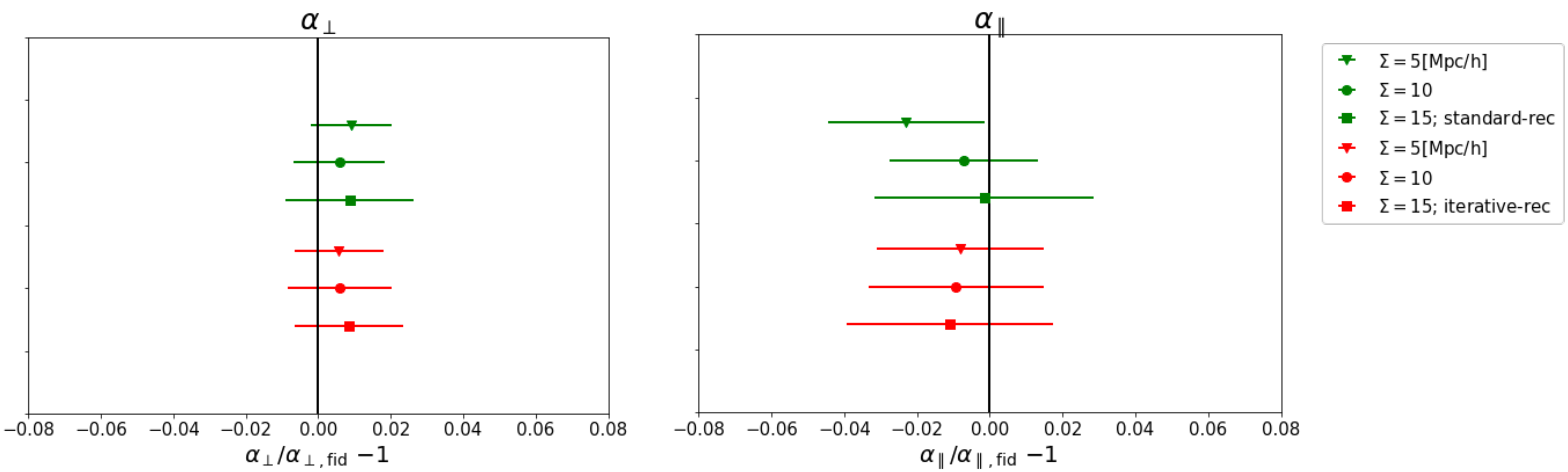

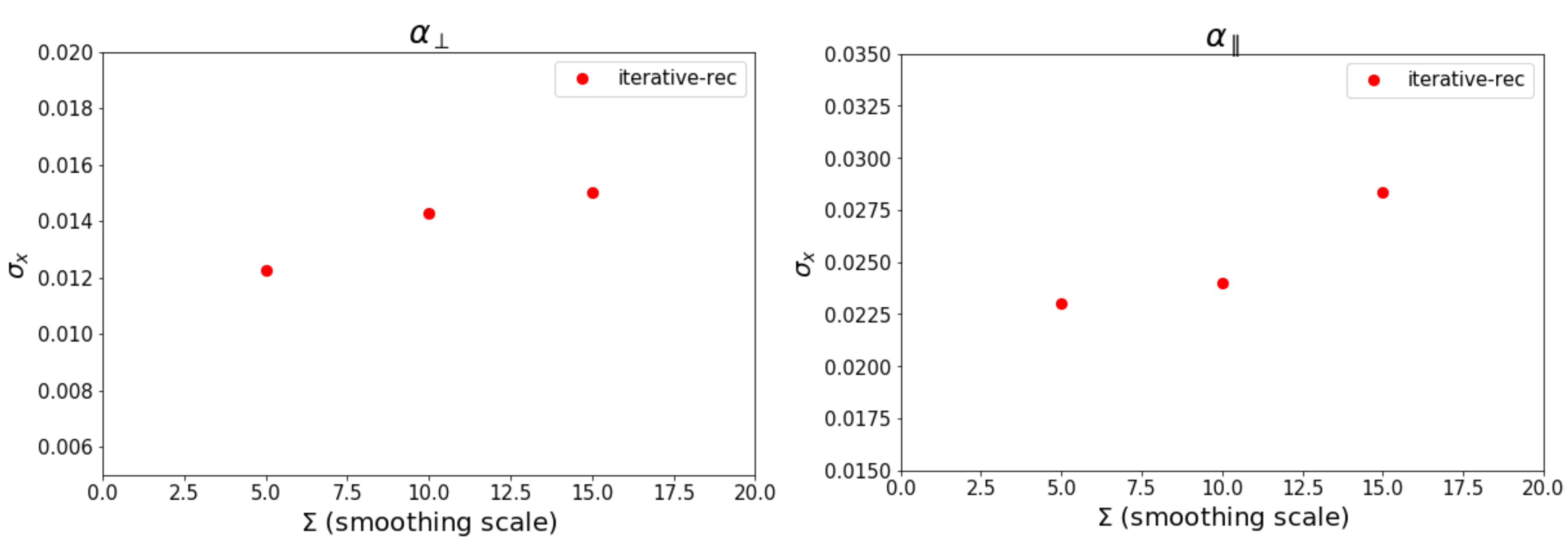

best fit values don't depend on the smoothing scale in the iterative method

with a smaller smoothing scale, the error gets smaller

Impact on the distance measurements

w/o nuisance parameters

perpendicular

$$\alpha_\perp = \frac{D_M(z) r_{d,\mathrm{fid}}}{D_M^{\mathrm{fid}}(z) r_d},$$

line-of-sight

$$\alpha_\parallel = \frac{H^{\mathrm{fid}}(z) r_{d,\mathrm{fid}}}{H(z) r_d}$$

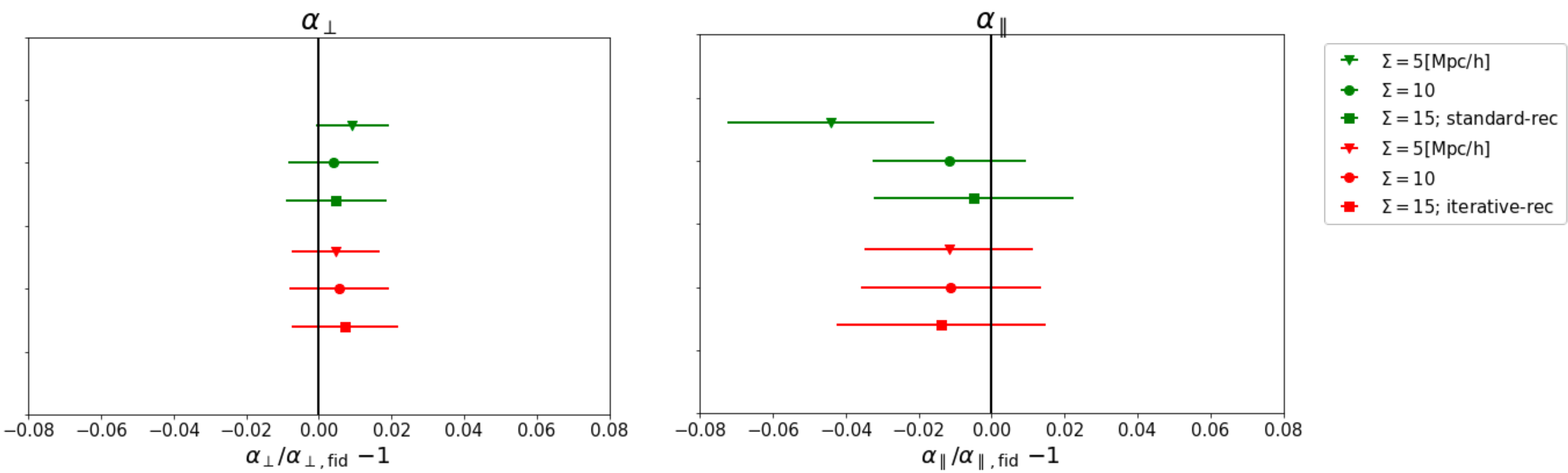

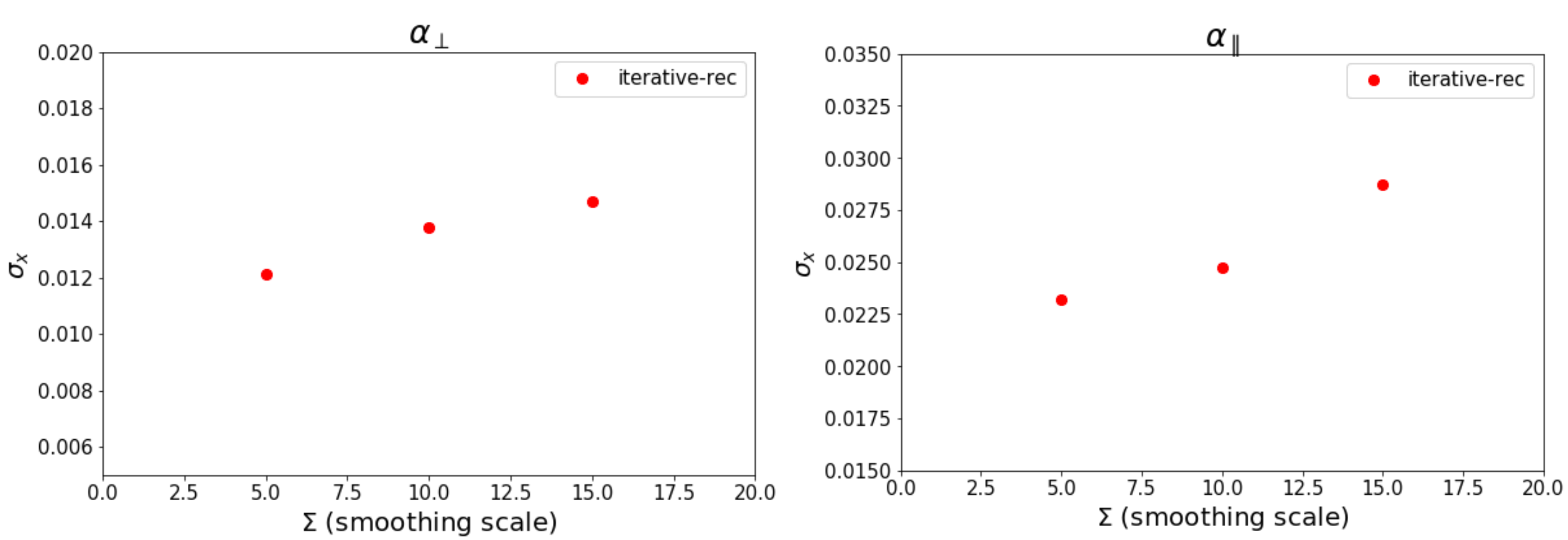

in the standard method, nuisance parameters compensate the difference in the smoothing scales

Summary

BAO is a powerful tool to measure the cosmological distance scale and understand the property of DE

reach more than 1% accuracy distance measurements in upcoming galaxy redshift surveys

developed an iterative reconstruction method to settle the problems in the standard reconstruction and applied it to galaxy mocks

correlation function can be reconstructed more precisely even on large scales (> 50 Mpc/h)

measured the distance scale using the reconstructed correlation function

the new iterative method is not impacted by the smoothing scale unlike the standard method

considering the effect of survey geometry or number density…

Backup slides

BAO peak degradation

Which scale is responsible for the differential motion ?

(Eisenstein+ 2007)

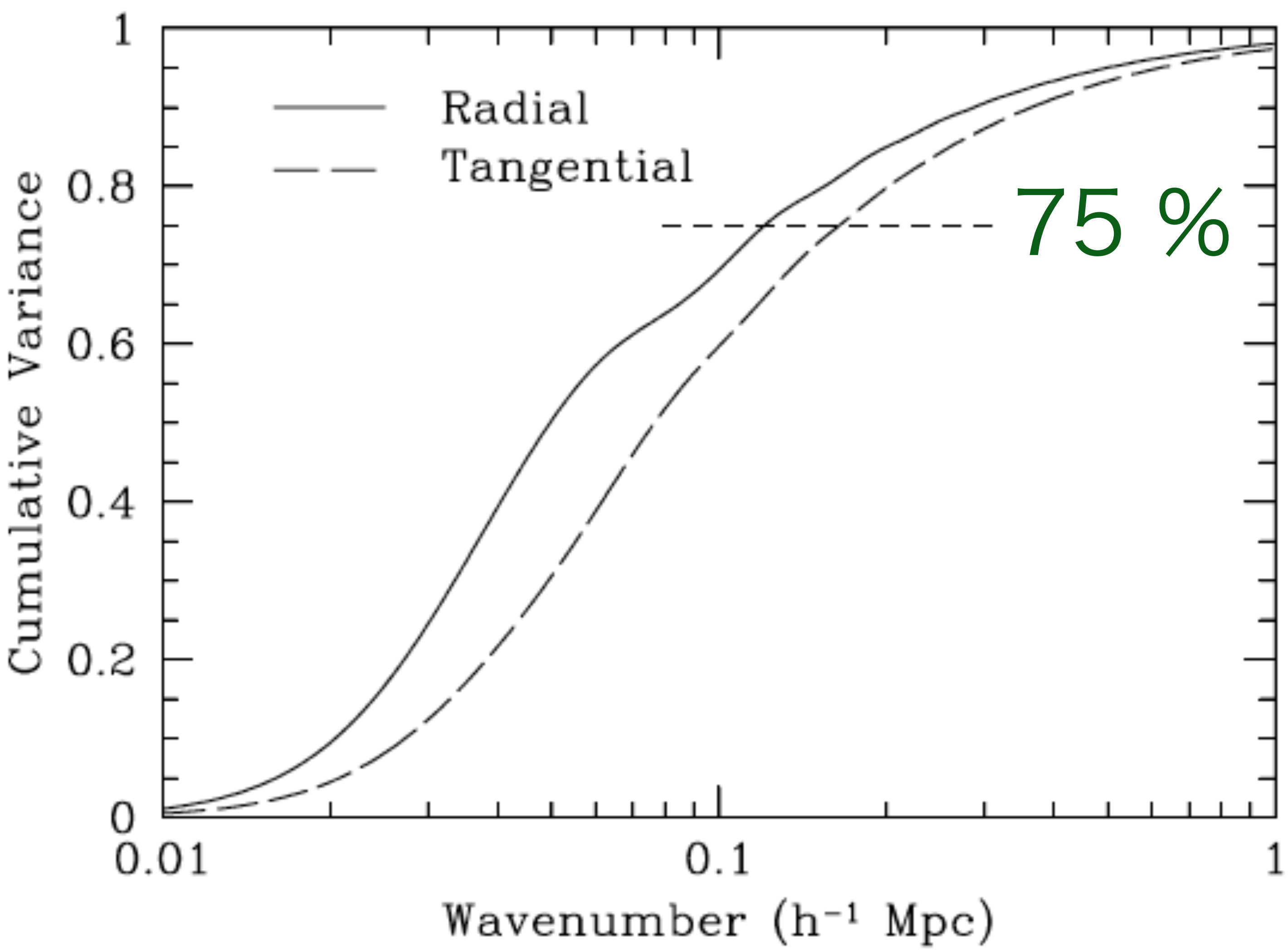

Cumulative variance in the differential motion of pairs initially separated by 150 Mpc as a function of cutoff wavenumber

LPT vs EPT (1st order)

Cross correlation with the non-linear density field

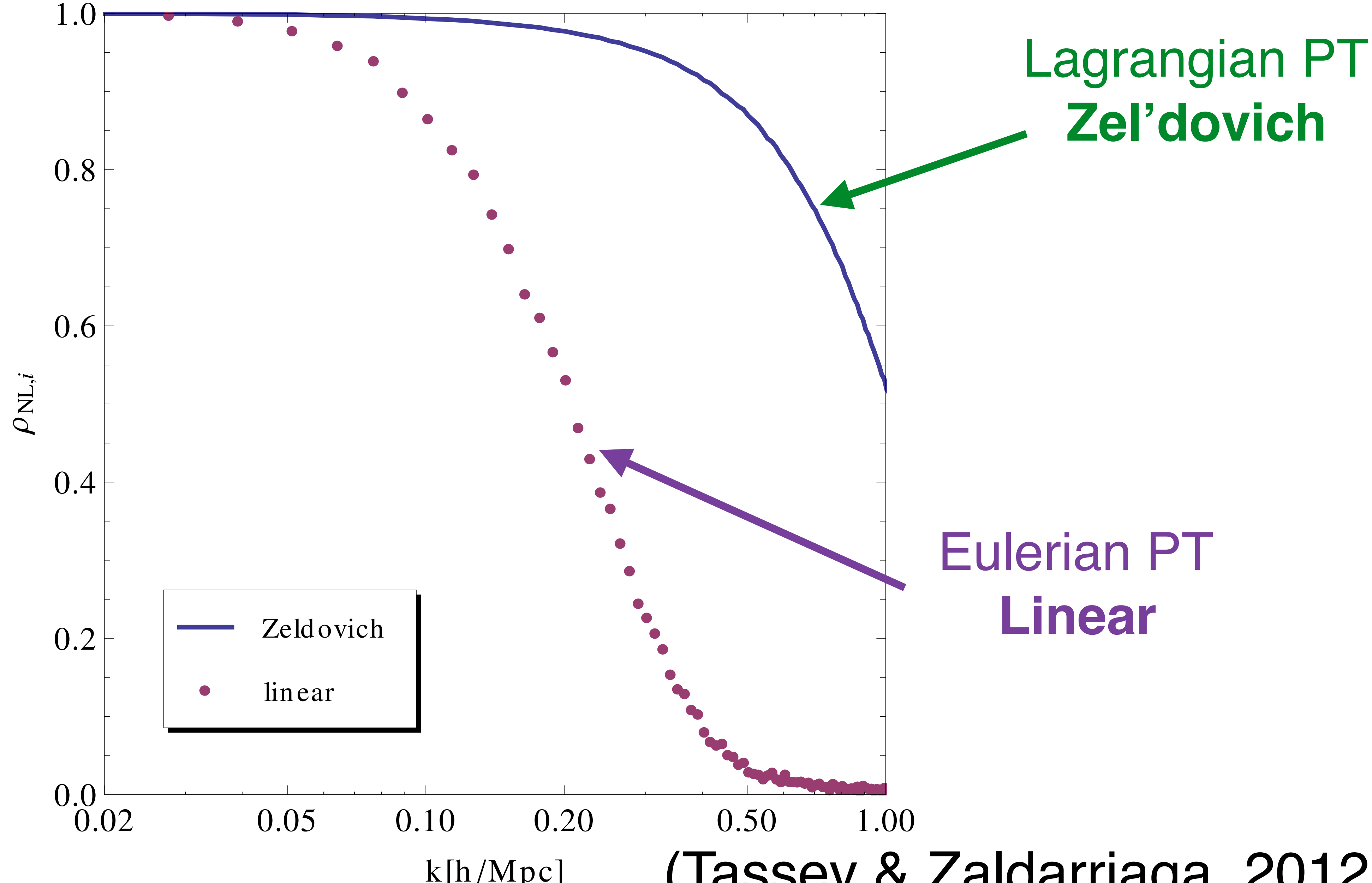

(Tassev & Zaldarriaga, 2012)

Up to the 1st order, Lagrangian PT is better

Application to N-body simulations

(**RH** & Eisenstein, 2018; 2019)

N-body simulation

Abacus (Garrison+ 2017), 20 boxes

Box size: 1100 [Mpc/h]
Number of particles: 1440^3
Redshift: z = 0.5

sampling → **Matter field** $N_{\rm p} \simeq 480^3$

Rockstar → **Halo fields** → **Galaxy fields** $N_{\rm p} \simeq 84^3$

GRAND-HOD
(Yuan+ 2018)

Reduction of smoothing scale

Initial scale: 20 [Mpc/h]

Final scale: 5, 10, 15 [Mpc/h]

$$\Sigma = \frac{\Sigma_{\rm ini}}{1.2^n}$$

n: the number of iteration

Convergence

$$\frac{\sum[\delta_{\rm L(n)} - \delta_{\rm L(n-1)}]^2}{\sum \delta_s^2} < 0.01$$

over all grid points

Galaxy as a biased tracer

(**RH** & Eisenstein, 2019)

	Matter		Galaxy
Density:	$\delta_s(\mathbf{s})$	$\longrightarrow$	$\delta_s(\mathbf{s})/b$
Linear growth rate:	f	$\longrightarrow$	$\beta = f/b$

Kaiser relation:

$$\tilde{\delta}^g_s(\mathbf{k}) = (1+\beta\mu^2)\tilde{\delta}^g(\mathbf{k})$$

where $\mu = k_z/k \quad \beta = f/b$

$$\underbrace{\delta^g}_{\text{galaxy}} = b\underbrace{\delta}_{\text{matter}}$$: Linear galaxy bias

Bias: $b = r_{i,\mathrm{gal}}(k_{\mathrm{cr}})/r_{i,\mathrm{mat}}(k_{\mathrm{cr}})$

where $r_i(k) \equiv \dfrac{\langle \tilde{\delta}\tilde{\delta}^*_{\mathrm{ini}}\rangle}{\langle |\tilde{\delta}_{\mathrm{ini}}|^2\rangle} \quad k_{\mathrm{cr}} = 0.1\ [h/\mathrm{Mpc}]$